

Supporting Information for

**Triaminoborane-Bridged Diphosphine Complexes with Ni and Pd:
Coordination Chemistry, Structures, and Ligand-Centered Reactivity**

Kyoungsoon Lee, Courtney M. Donahue, Scott R. Daly*

The University of Iowa, Department of Chemistry, E331 Chemistry Building, Iowa City, IA
52242-1294

Table of Contents

| | |
|--------------------------|------------|
| Molecular Structure of 3 | pp. 2 |
| Crystallographic Data | pp. 3 – 4 |
| NMR Spectra | pp. 5 – 56 |

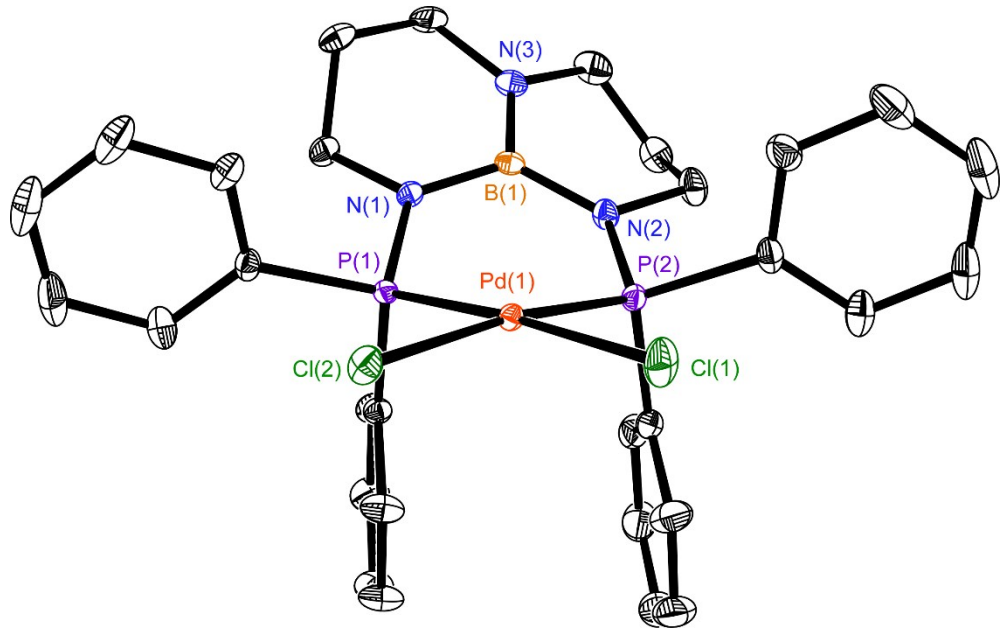


Figure S1. Molecular structure of $(^{\text{Ph}}\text{TBDPhos})\text{PdCl}_2$ (3) with thermal ellipsoids at the 35% probability level. Hydrogen atoms were omitted from the figure.

Table S1. Crystallographic data for ^{Ph}TBDPhos, ^{iPr}TBDPhos, (^{Ph}TBDPhos)NiCl₂ (**1**), (^{iPr}TBDPhos)NiCl₂ (**2**), (^{Ph}TBDPhos)PdCl₂ (**3**), and (^{iPr}TBDPhos)PdCl₂ (**4**).

| | ^{Ph} TBDPhos | ^{iPr} TBDPhos | 1 | 2 | 3 | 4 |
|--|--|--|---|--|---|---|
| formula | C ₃₂ H ₃₆ BCl ₄ N ₃ P ₂ | C ₁₈ H ₄₀ BN ₃ P ₂ | C ₁₆ H ₁₇ B _{0.5} Cl ₄ N _{1.5} Ni _{0.5} P | C ₁₈ H ₄₀ BCl ₂ N ₃ NiP ₂ | C ₃₀ H ₃₂ BCl ₂ N ₃ P ₂ Pd | C ₁₈ H ₄₀ BCl ₂ N ₃ P ₂ Pd |
| FW (g mol ⁻¹) | 677.19 | 371.28 | 437.75 | 500.89 | 684.63 | 548.58 |
| crystal system | Monoclinic | Monoclinic | Triclinic | Monoclinic | Monoclinic | Monoclinic |
| space group | C2/c | P2 ₁ /c | P-1 | C2/c | P2 ₁ /c | P2 ₁ /n |
| a (Å) | 22.219(2) | 8.6254(9) | 9.9895(10) | 12.6274(13) | 12.9178(13) | 8.8840(9) |
| b (Å) | 13.6886(14) | 15.2128(15) | 12.2230(12) | 10.9057(11) | 13.3011(13) | 17.2077(17) |
| c (Å) | 13.9571(14) | 17.6220(18) | 16.8174(17) | 17.6347(18) | 18.1092(18) | 16.0964(16) |
| α (deg) | 90 | 90 | 90.040(5) | 90 | 90 | 90 |
| β (deg) | 127.323(5) | 101.400(5) | 103.664(5) | 101.618(5) | 104.019(5) | 94.786(5) |
| γ (deg) | 90 | 90 | 106.259(5) | 90 | 90 | 90 |
| volume (Å ³) | 3375.8(6) | 2266.7(4) | 1910.6(3) | 2378.7(4) | 3018.9(5) | 2452.1(4) |
| Z | 8 | 4 | 4 | 4 | 4 | 4 |
| ρ _{calc} (g cm ⁻³) | 1.332 | 1.088 | 1.522 | 1.399 | 1.506 | 1.486 |
| μ (mm ⁻¹) | 0.473 | 0.197 | 1.179 | 1.184 | 0.923 | 1.115 |
| F(000) | 1408 | 816 | 892 | 1064 | 1392 | 1136 |
| θ range (deg) | 2.92/27.37 | 2.93/27.94 | 2.45/27.41 | 2.49/26.36 | 2.92/29.04 | 2.59/27.97 |
| R(int) | 0.0440 | 0.0574 | 0.0500 | 0.0309 | 0.0294 | 0.0351 |
| data/restraints/parameters | 4062/0/191 | 5424/0/225 | 8798/0/426 | 2444/0/128 | 8050/0/352 | 5882/0/252 |
| GOF | 1.050 | 1.021 | 1.026 | 1.035 | 1.079 | 1.023 |
| R ₁ [<i>I</i> > 2σ(<i>I</i>)] ^a | 0.0331 | 0.0369 | 0.0355 | 0.0239 | 0.0233 | 0.0245 |
| wR ₂ (all data) ^b | 0.0872 | 0.0998 | 0.0941 | 0.0578 | 0.0558 | 0.0577 |
| Ext. Coeff | - | - | - | - | - | - |
| Largest Peak/Hole (e·Å ⁻³) | 0.372/-0.372 | 0.399/-0.265 | 0.889/-0.943 | 0.320/-0.224 | 0.439/-0.422 | 0.470/-0.329 |
| Temp (K) | 190(2) | 190(2) | 190(2) | 190(2) | 190(2) | 190(2) |

^aR₁ = $\sum |F_o| - |F_c| | / | \sum |F_o|$ for reflections with $F_o^2 > 2 \sigma(F_o^2)$.

^bwR₂ = $[\sum w(F_o^2 - F_c^2)^2 / \sum (F_o^2)^2]^{1/2}$ for all reflections.

Table S2. Crystallographic data for $\{[({}^{\text{Ph}}\text{TBDPhos}-\text{H}_2\text{O})\text{Ni}]_2(\mu\text{-OH})_2\}\text{Cl}_2$ (**5**), $({}^{\text{Ph}}\text{TBDPhos}-\text{MeOH})\text{NiCl}_2$ (**7**), $({}^{\text{Ph}}\text{TBDPhos}-\text{MeOH})\text{PdCl}_2$ (**8**), $({}^{\text{Ph}}\text{TBDPhos}-\text{C}_3\text{H}_5\text{OH})\text{PdCl}_2$ (**9**), and $\{[({}^{\text{Ph}}\text{TBDPhos}-\text{HF})\text{Ni}]_2(\mu\text{-OH})_2\}\text{Cl}_2$ (**10**).

| | 5 | 7 | 8 | 9 | 10 |
|--|--|--|--|--|--|
| formula | C ₃₀ H ₃₅ BClN ₃ NiO ₂ P | C ₃₁ H ₃₆ BCl ₂ N ₃ NiOP | C ₃₁ H ₃₆ BCl ₂ N ₃ OP ₂ Pd | C ₃₃ H ₃₈ BCl ₂ N ₃ OP ₂ Pd | C ₆₂ H ₇₂ B ₂ Cl ₆ F ₂ N ₆ Ni ₂ O ₂ P ₄ |
| FW (g mol ⁻¹) | 636.52 | 668.99 | 716.68 | 742.71 | 964.58 |
| crystal system | Monoclinic | Monoclinic | Monoclinic | Monoclinic | Monoclinic |
| space group | P2 ₁ /n | P2 ₁ /c | P2 ₁ /c | P2 ₁ /c | P2 ₁ /n |
| a (Å) | 13.8071(14) | 10.9172(11) | 10.9956(11) | 10.8193(11) | 12.3721(12) |
| b (Å) | 11.3545(11) | 21.128(2) | 21.129(2) | 22.229(2) | 32.375(3) |
| c (Å) | 20.486(2) | 14.1842(14) | 14.3055(14) | 14.5574(15) | 16.7696(17) |
| α (deg) | 90 | 90 | 90 | 90 | 90 |
| β (deg) | 106.374(5) | 110.222(5) | 110.691(5) | 110.787(5) | 91.629(5) |
| γ (deg) | 90 | 90 | 90 | 90 | 90 |
| volume (Å ³) | 3081.4(5) | 3070.0(5) | 3109.2(5) | 3273.2(6) | 6714.3(11) |
| Z | 4 | 4 | 4 | 4 | 4 |
| ρ _{calc} (g cm ⁻³) | 1.372 | 1.447 | 1.531 | 1.507 | 1.431 |
| μ (mm ⁻¹) | 0.852 | 0.941 | 0.902 | 0.860 | 0.948 |
| F(000) | 1328 | 1392 | 1464 | 1520 | 2992 |
| θ range (deg) | 1.00/25.35 | 2.46/24.33 | 2.24/29.03 | 2.21/28.33 | 2.25/27.81 |
| R(int) | 0.0718 | 0.0739 | 0.0466 | 0.0241 | 0.0471 |
| data/restraints/parameters | 5637/3/373 | 6368/0/372 | 7766/0/375 | 8150/0/400 | 15831/1/783 |
| GOF | 0.881 | 0.912 | 1.039 | 1.056 | 0.855 |
| R ₁ [$I > 2\sigma(I)$] ^a | 0.0391 | 0.0408 | 0.0334 | 0.0212 | 0.0378 |
| wR ₂ (all data) ^b | 0.1320 | 0.1391 | 0.1263 | 0.0564 | 0.0985 |
| Ext. Coeff | - | 0.0020(6) | - | - | - |
| Largest Peak/Hole (e·Å ⁻³) | 0.290/-0.340 | 0.564/-0.589 | 1.032/-0.973 | 0.425/-0.398 | 1.097/-1.203 |
| Temp (K) | 190(2) | 190(2) | 190(2) | 170(2) | 190(2) |

^aR₁ = $\sum |F_o| - |F_c| | / | \sum |F_o|$ for reflections with $F_o^2 > 2 \sigma(F_o^2)$.

^bwR₂ = $[\sum w(F_o^2 - F_c^2)^2 / \sum (F_o^2)^2]^{1/2}$ for all reflections.

NMR Spectra

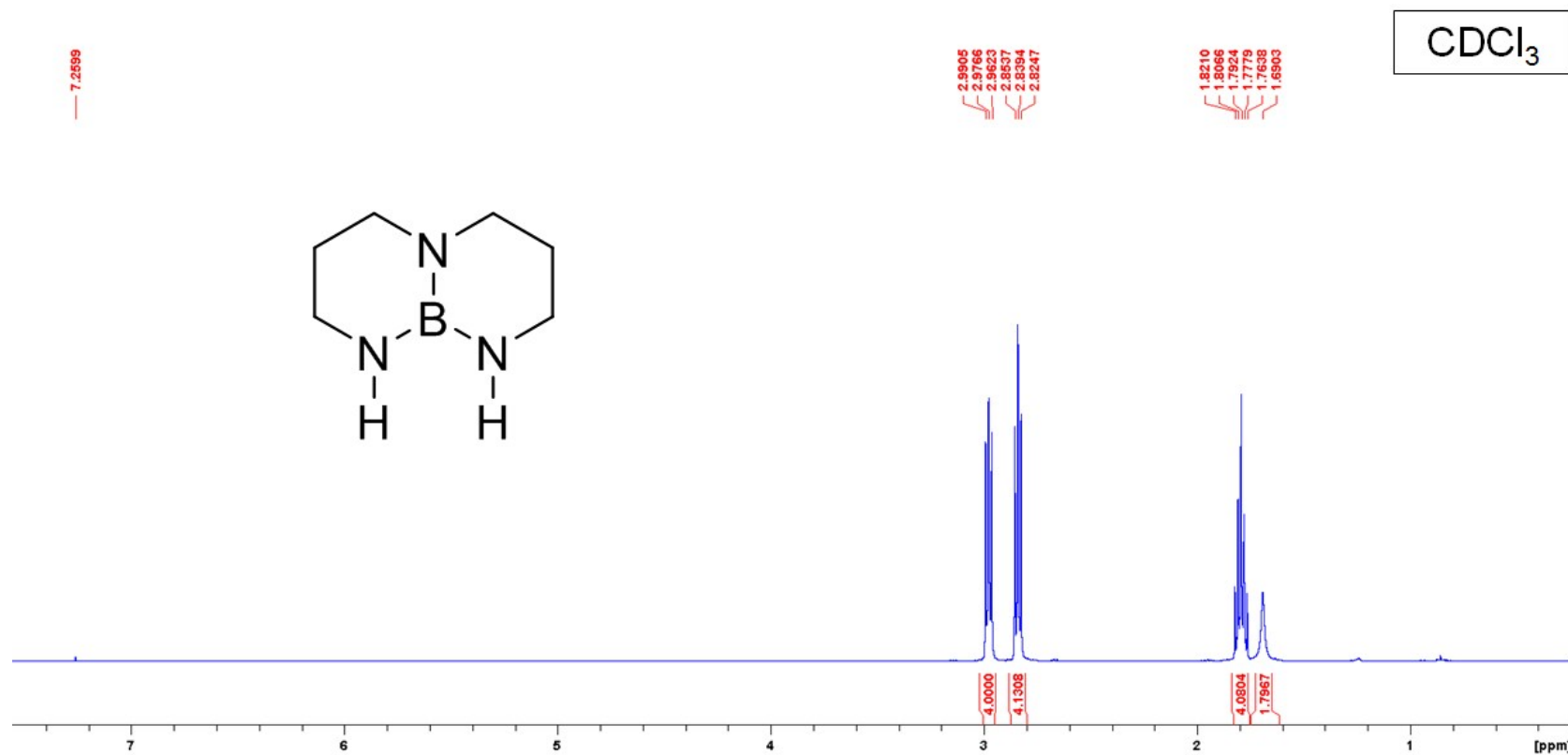


Figure S2. ^1H NMR spectrum of TBD.

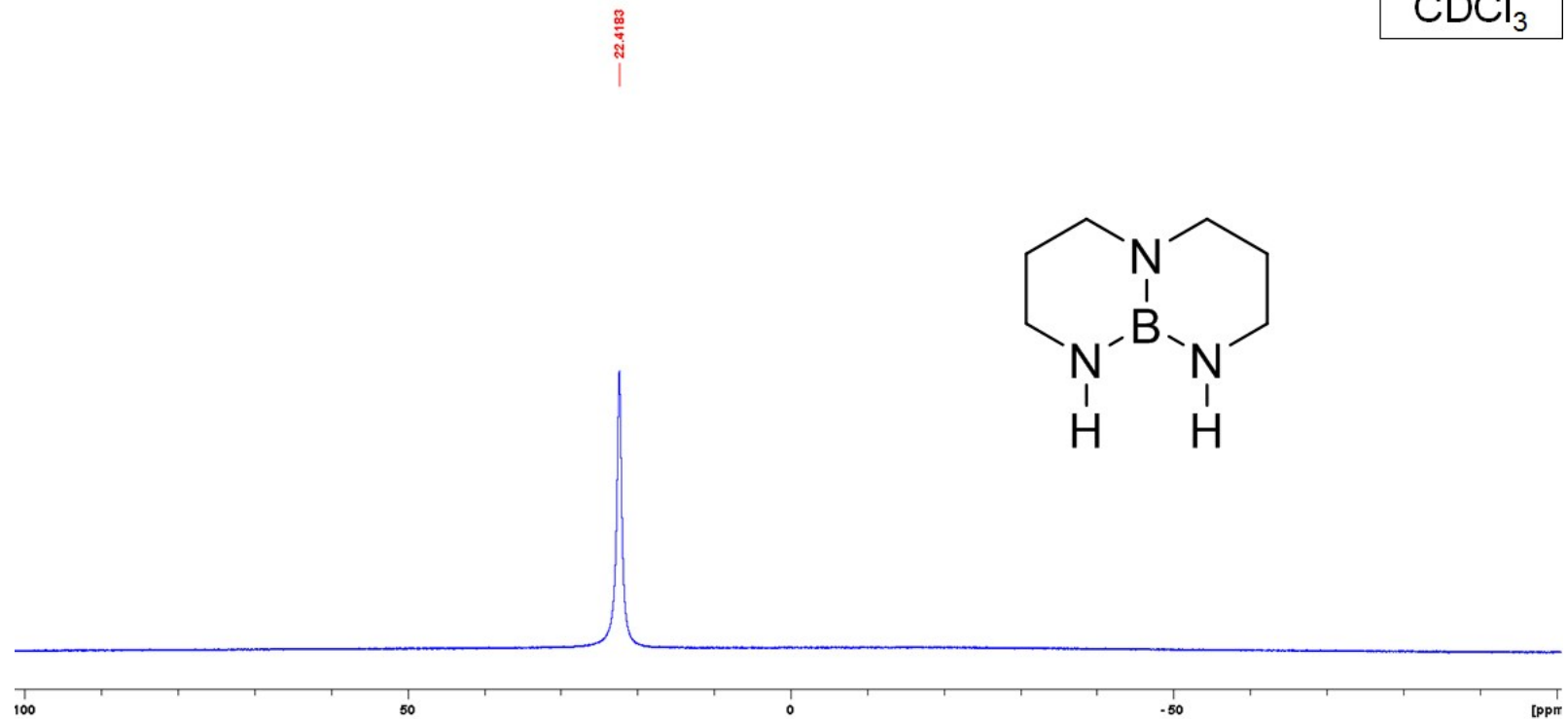


Figure S3. ^{11}B NMR spectrum of TBD.

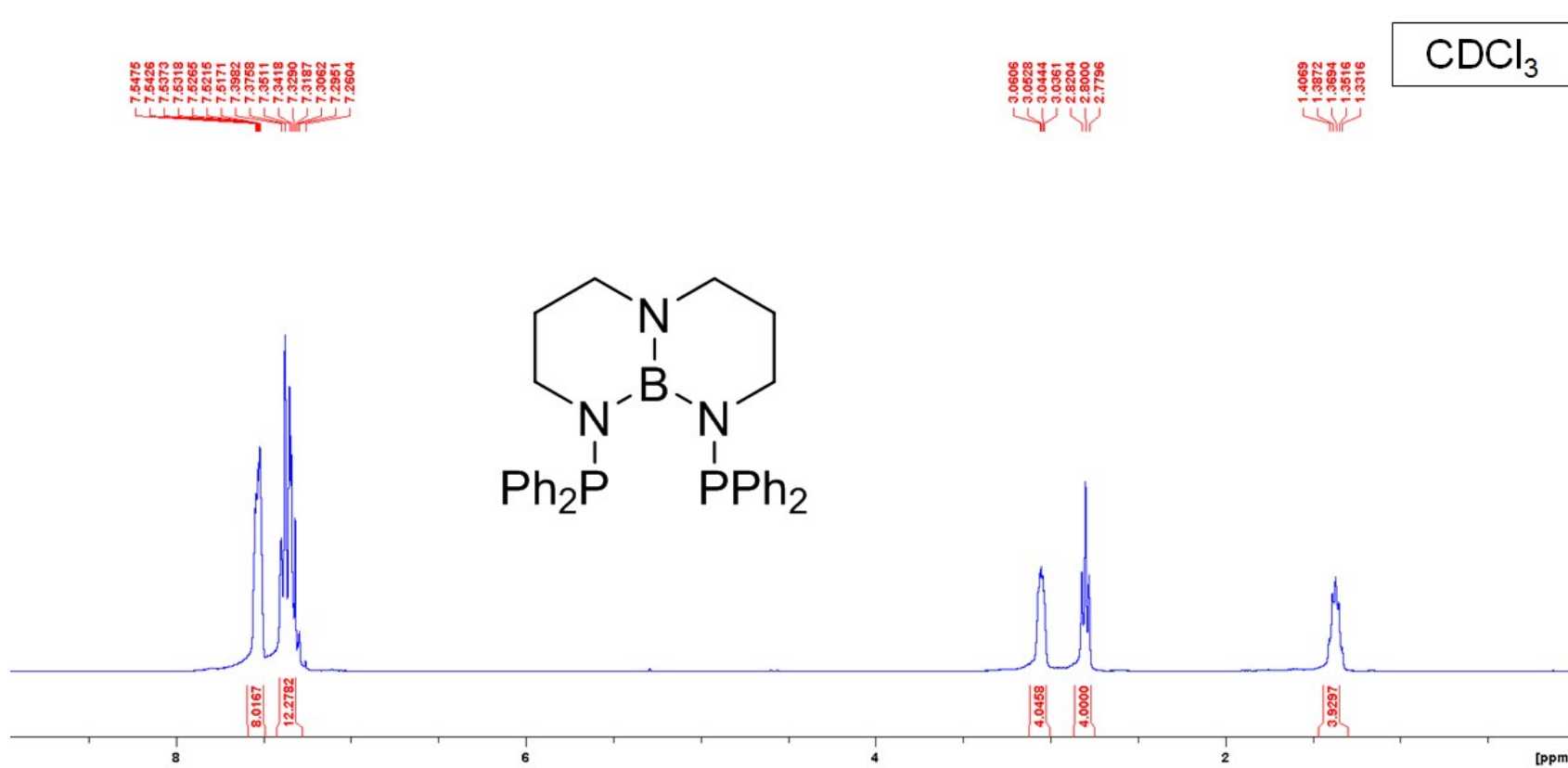


Figure S4. ¹H NMR spectrum of ^{Ph}TBDPhos.

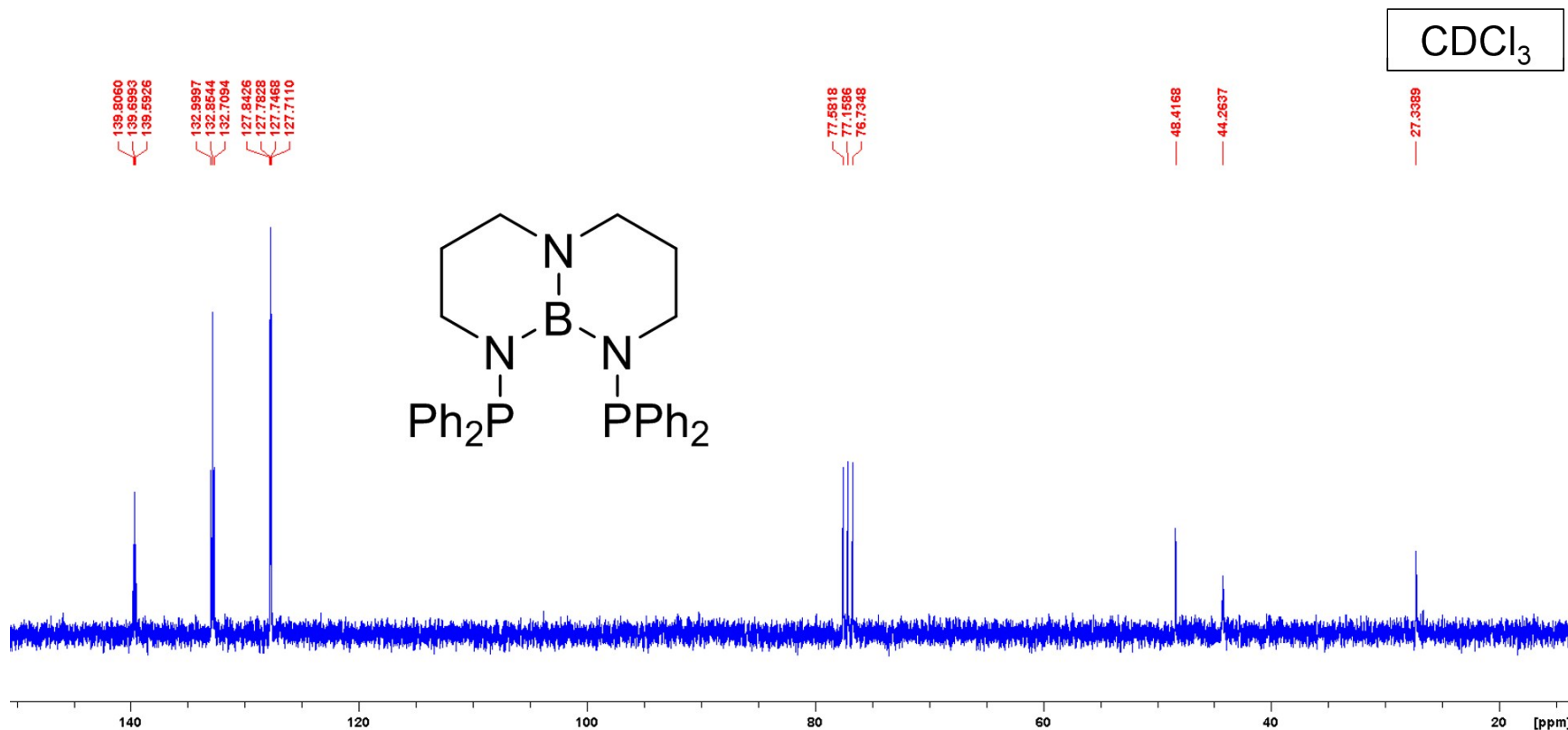


Figure S5. ^{13}C NMR spectrum of $^{\text{Ph}}\text{TBDPhos}$.

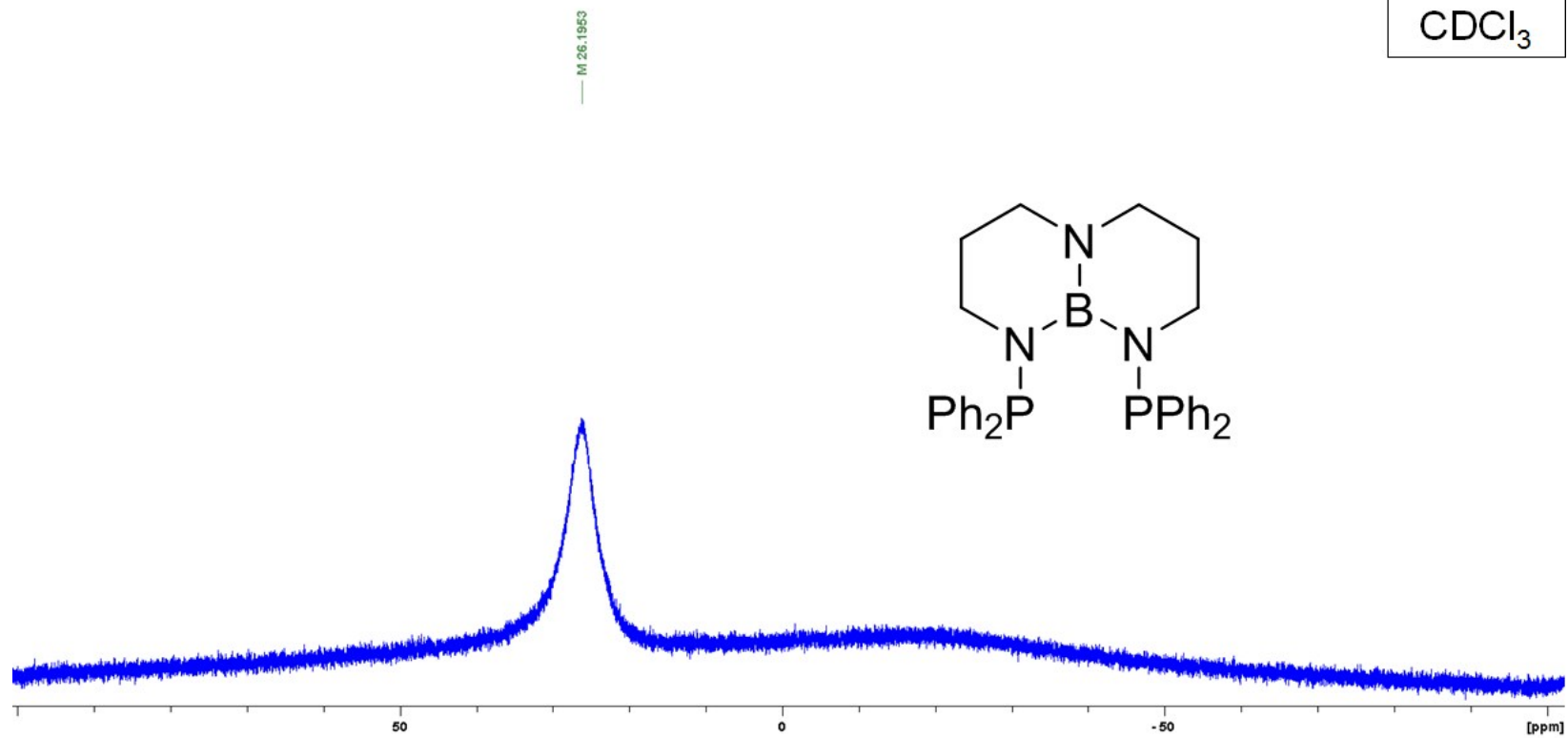


Figure S6. ^{11}B NMR spectrum of $^{\text{Ph}}\text{TBDPhos}$

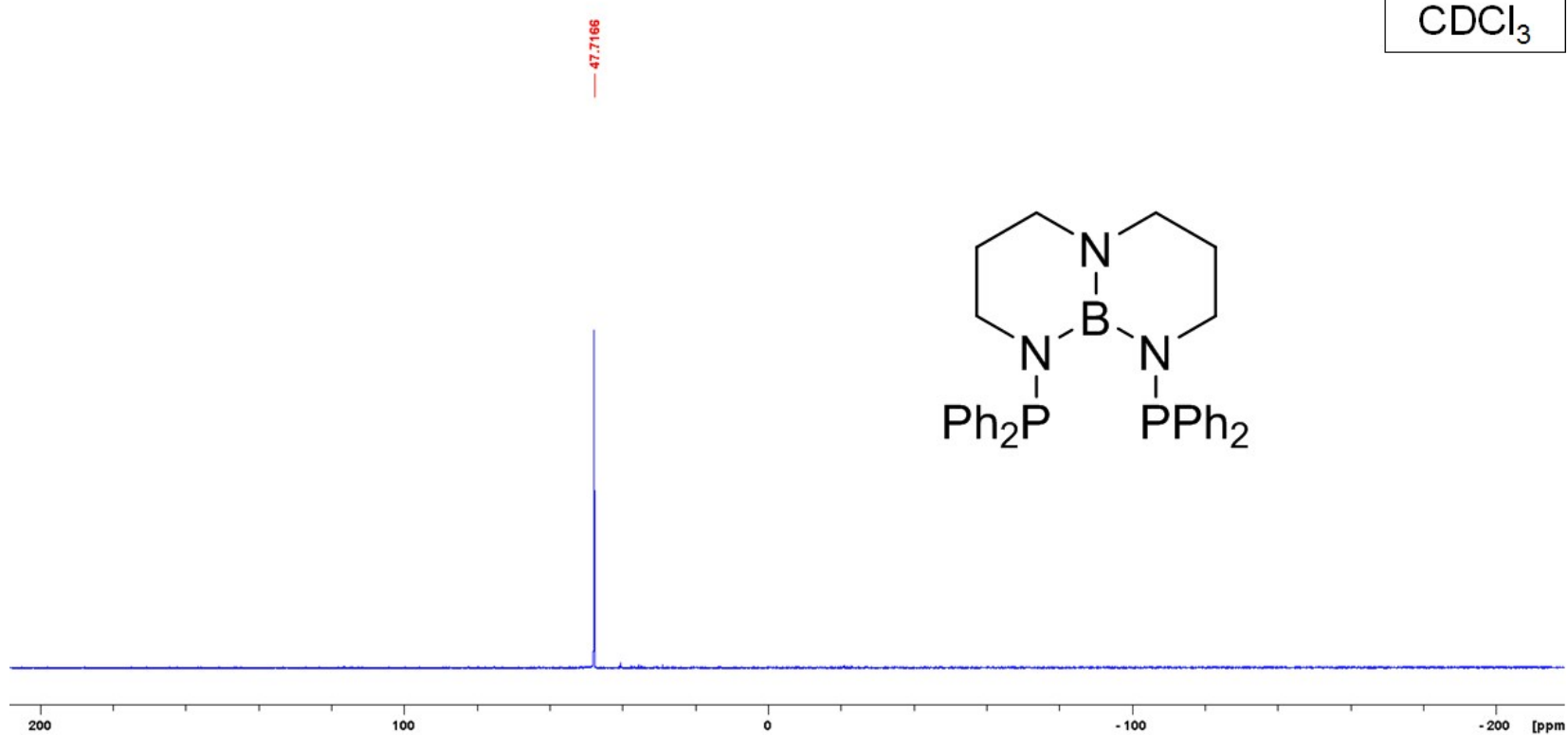


Figure S7. $^{31}\text{P}\{^1\text{H}\}$ NMR spectrum of $^{\text{Ph}}\text{TBDPhos}$.

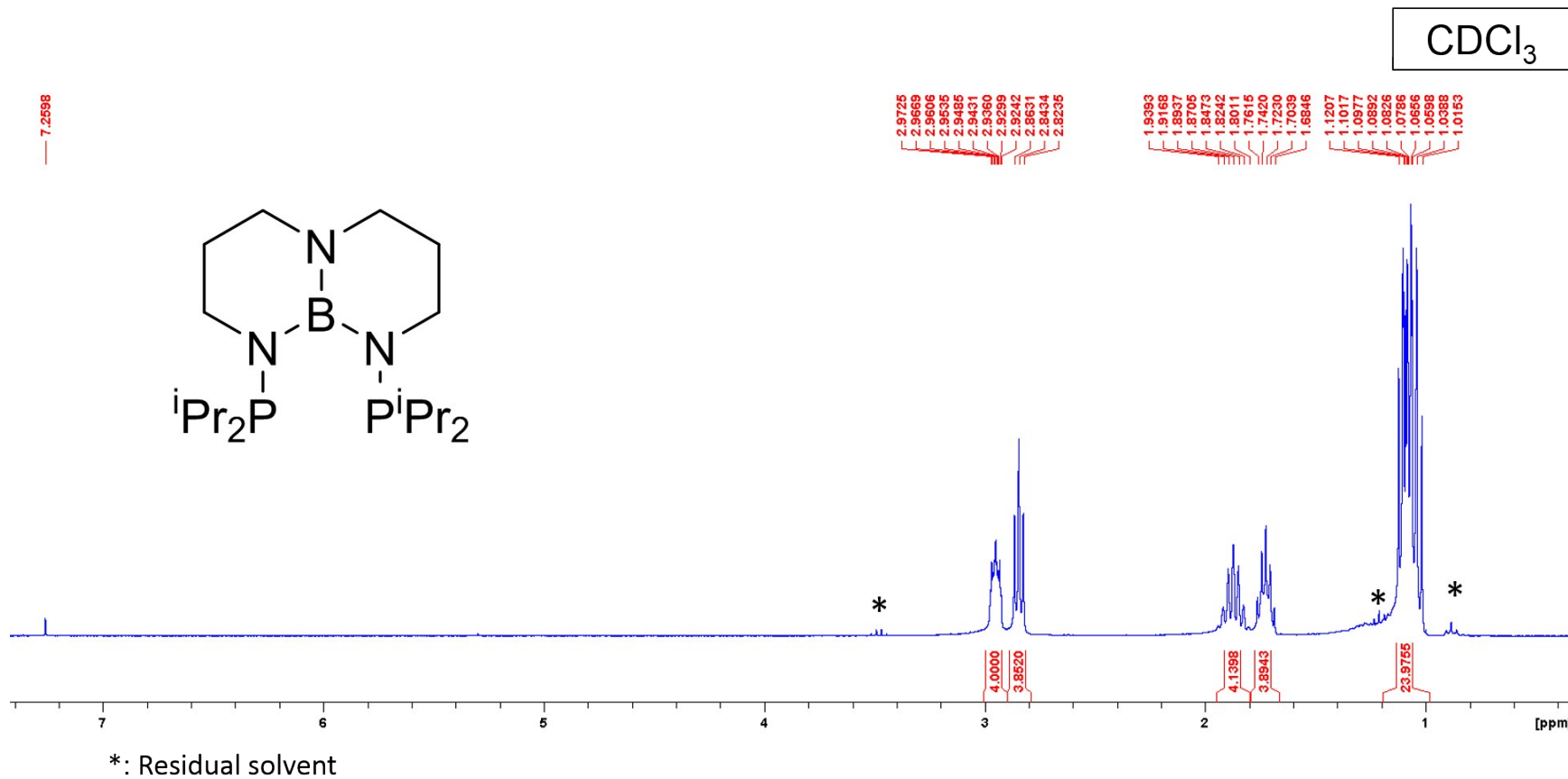


Figure S8. ¹H NMR spectrum of iPrTBDPhos. The * symbol indicates resonances assigned to residual Et₂O and pentane solvent.

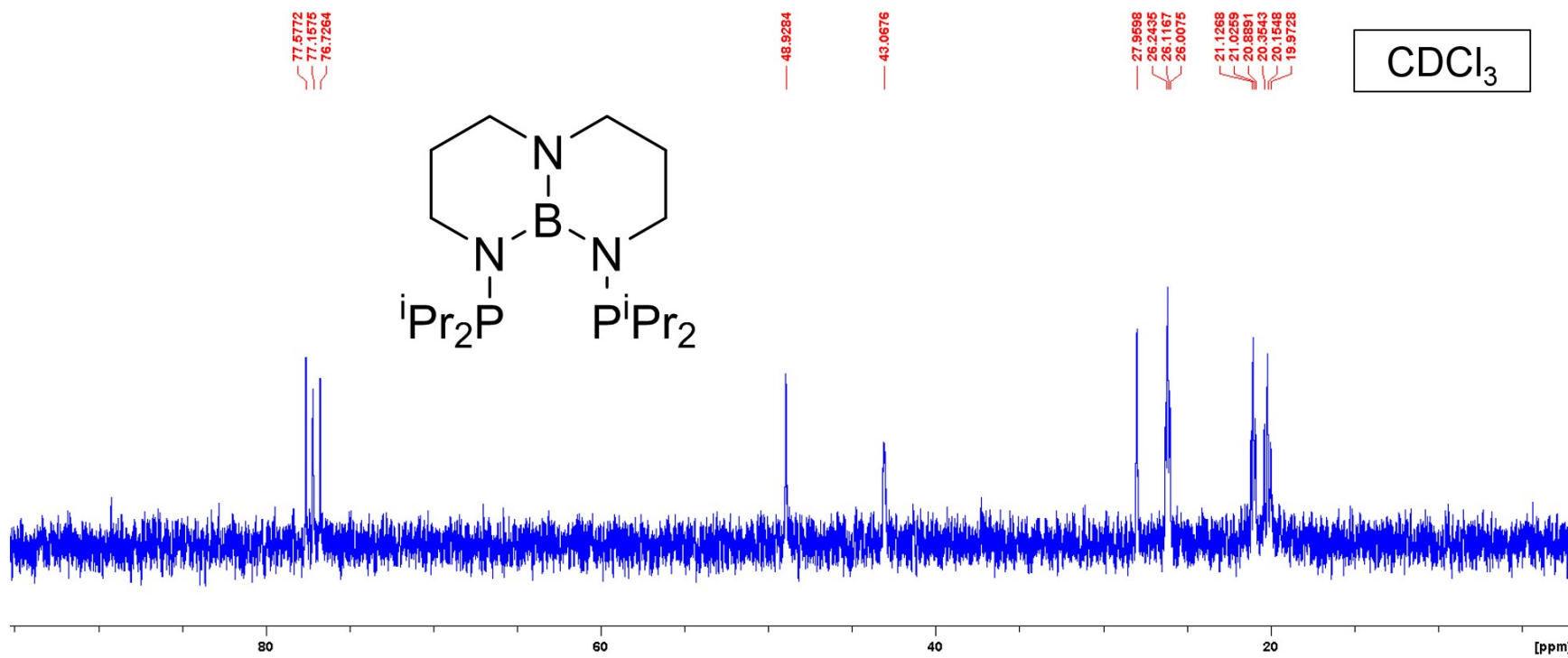


Figure S9. ^{13}C NMR spectrum of iPrTBDPhos .

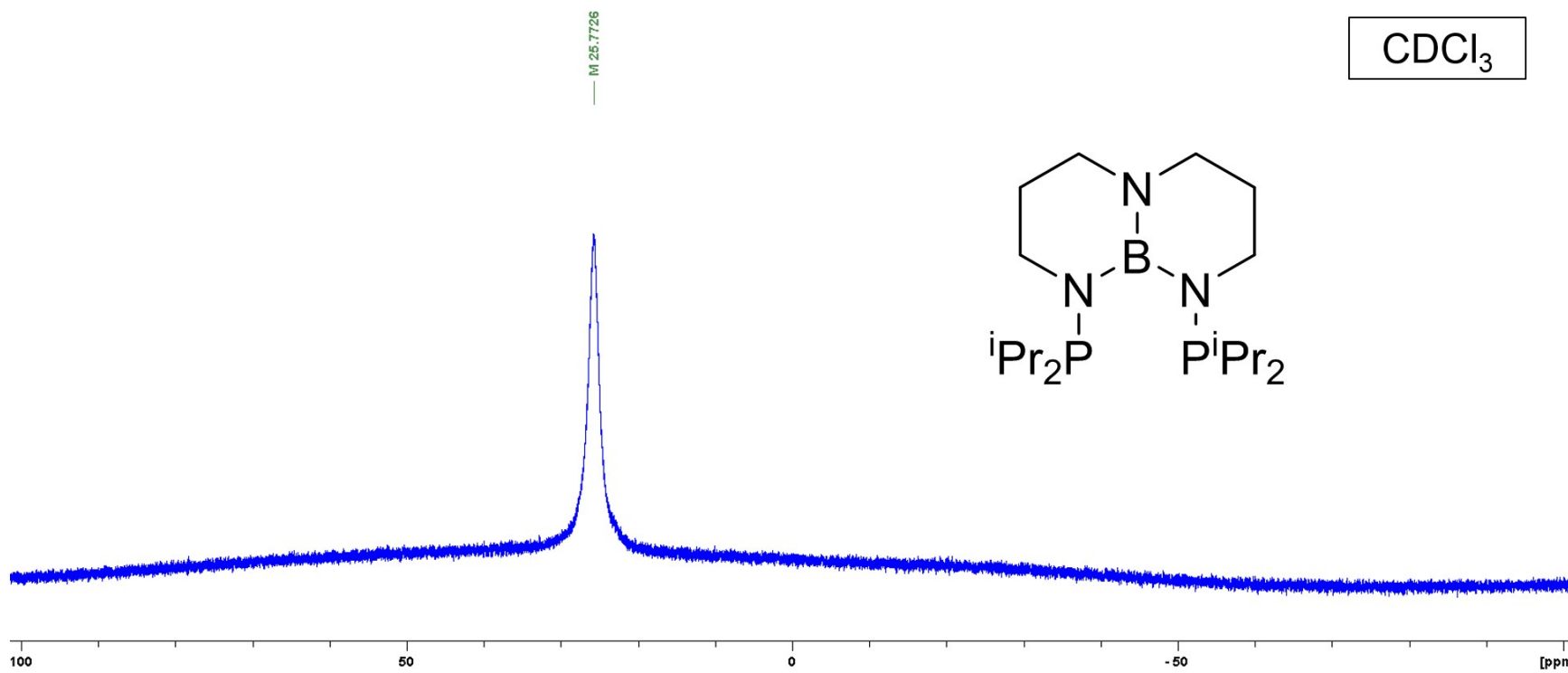


Figure S10. ¹¹B NMR spectrum of ⁱPrTBDPhos.

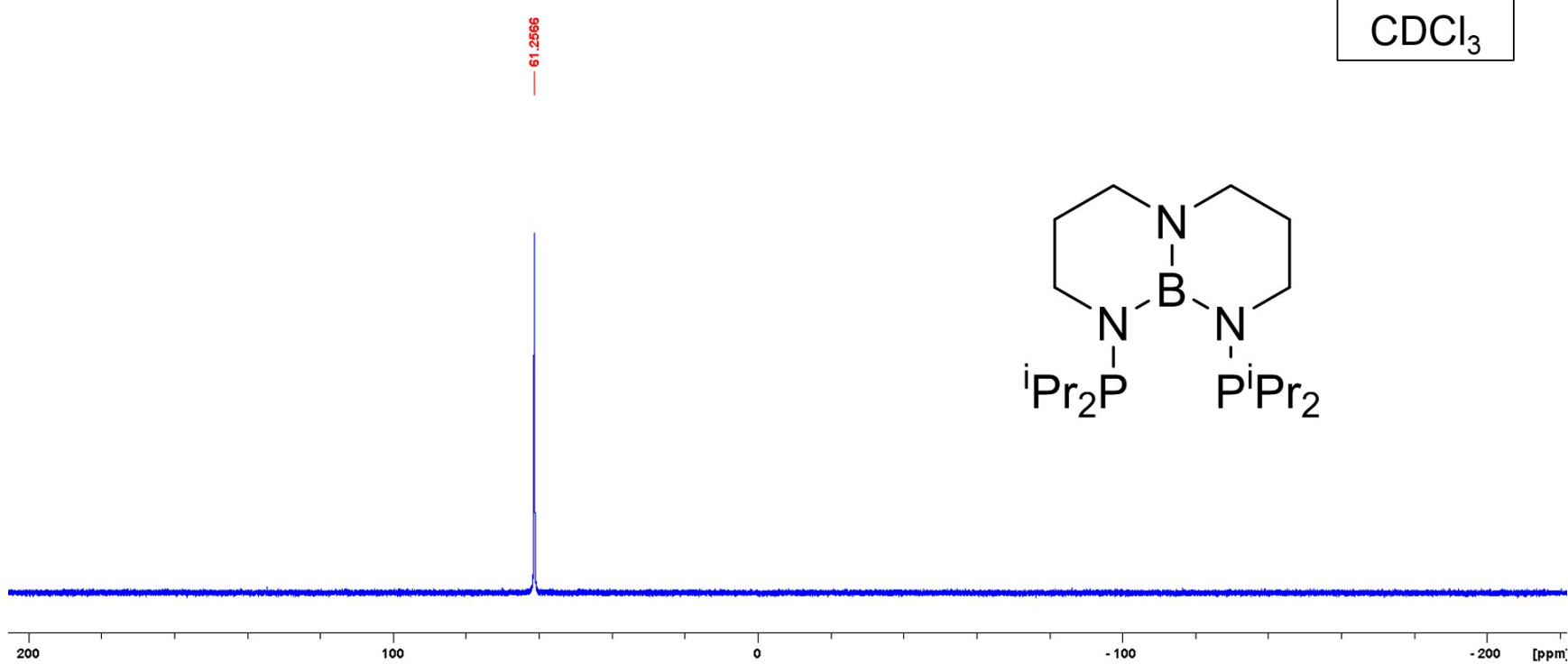


Figure S11. $^{31}\text{P}\{^1\text{H}\}$ NMR spectrum of iPrTBDPhos .

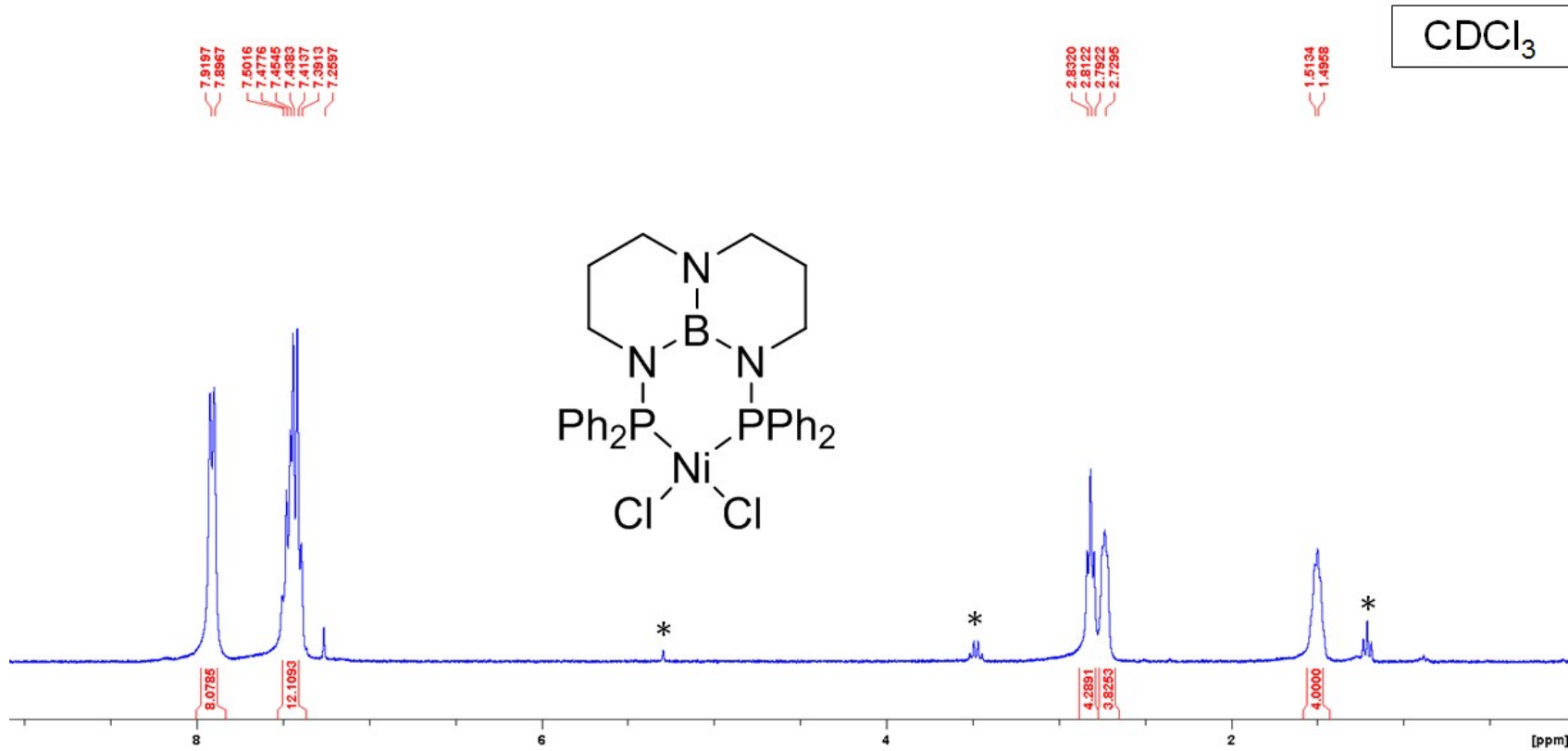


Figure S12. ^1H NMR spectrum of ($^{\text{Ph}}\text{TBDPhos}$) NiCl_2 (**1**). The * symbol indicates resonances assigned to residual CH_2Cl_2 and Et_2O solvent.

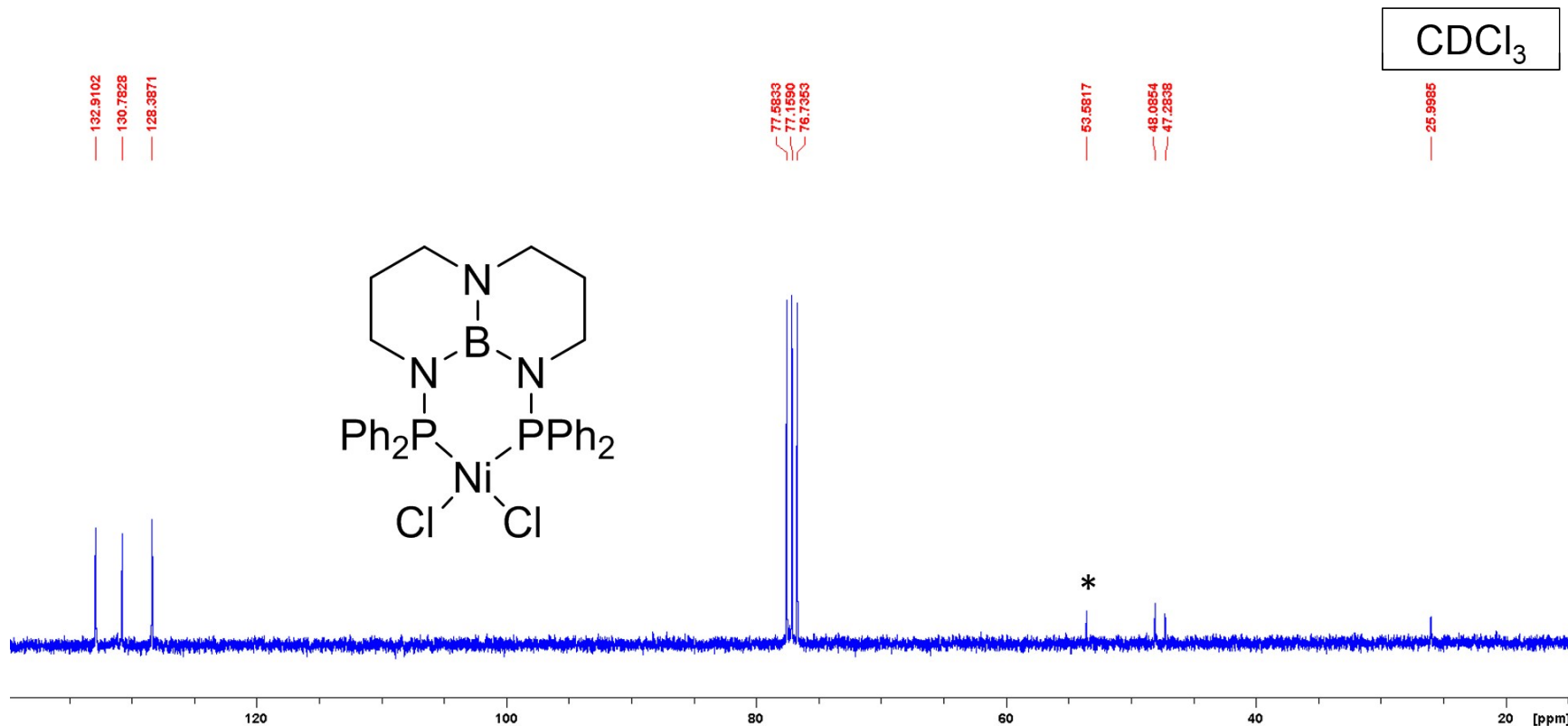


Figure S13. ^{13}C NMR spectrum of ($^{\text{Ph}}\text{TBDPhos}$)NiCl₂ (**1**). The * symbol indicates a resonance assigned to residual CH₂Cl₂ solvent.

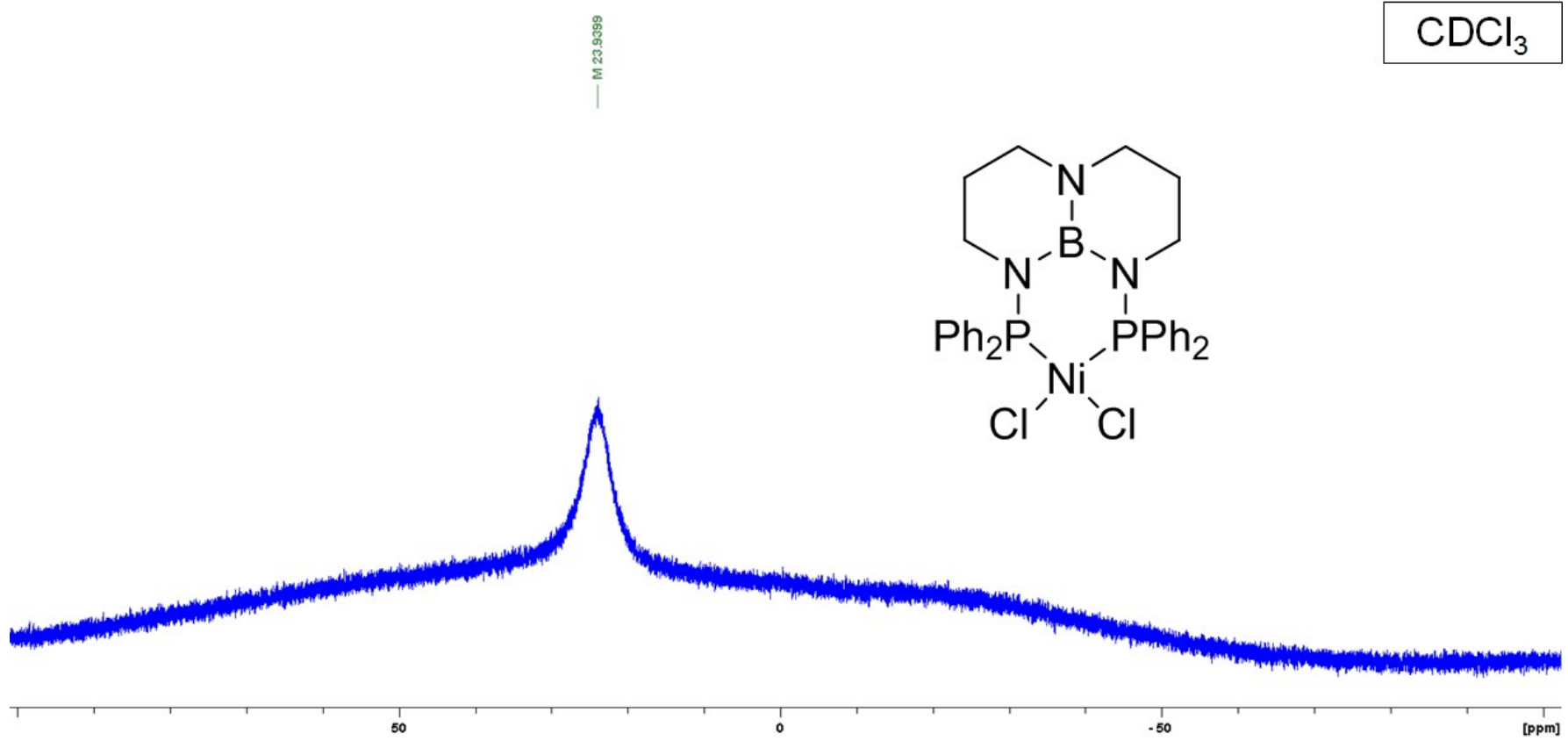


Figure S14. ¹¹B NMR spectrum of (^{Ph}TBDPhos)NiCl₂ (**1**).

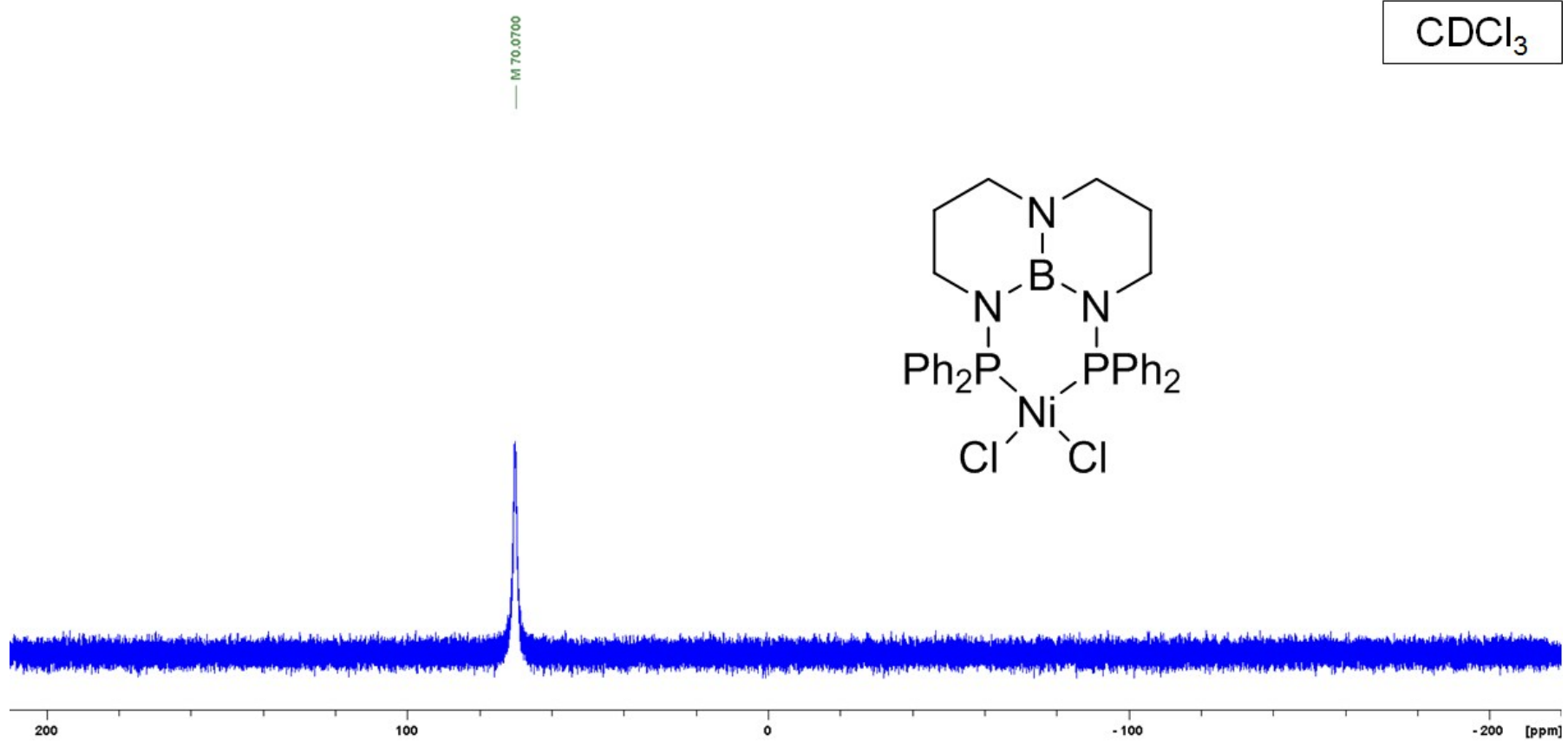


Figure S15. $^{31}\text{P}\{^1\text{H}\}$ NMR spectrum of $(^{\text{Ph}}\text{TBDPhos})\text{NiCl}_2$ (**1**).

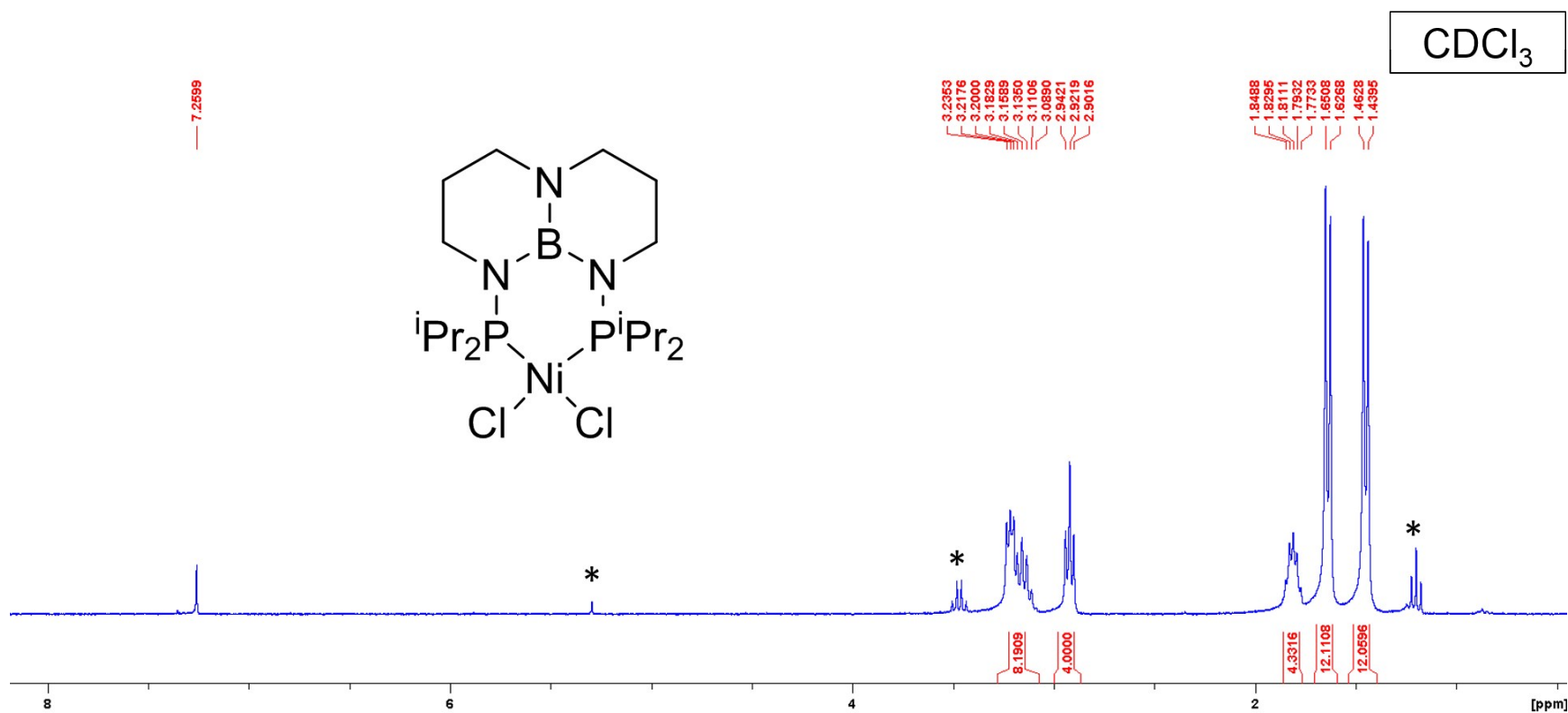


Figure S16. ¹H NMR spectrum of (ⁱPrTBDPhos)NiCl₂ (**2**). The * symbol indicates resonances assigned to residual CH₂Cl₂ and Et₂O solvent.

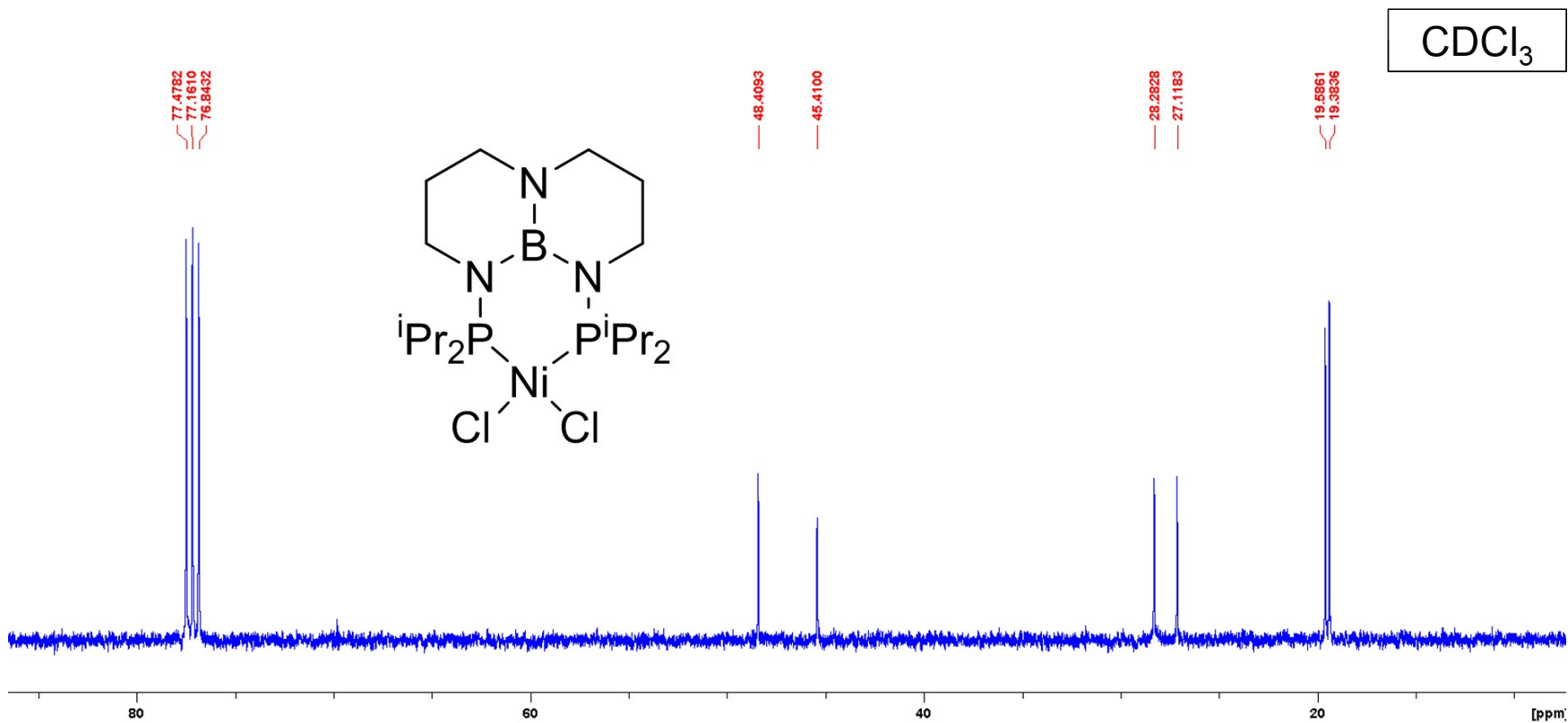


Figure S17. ^{13}C NMR spectrum of $(\text{iPrTBDPhos})\text{NiCl}_2$ (2).

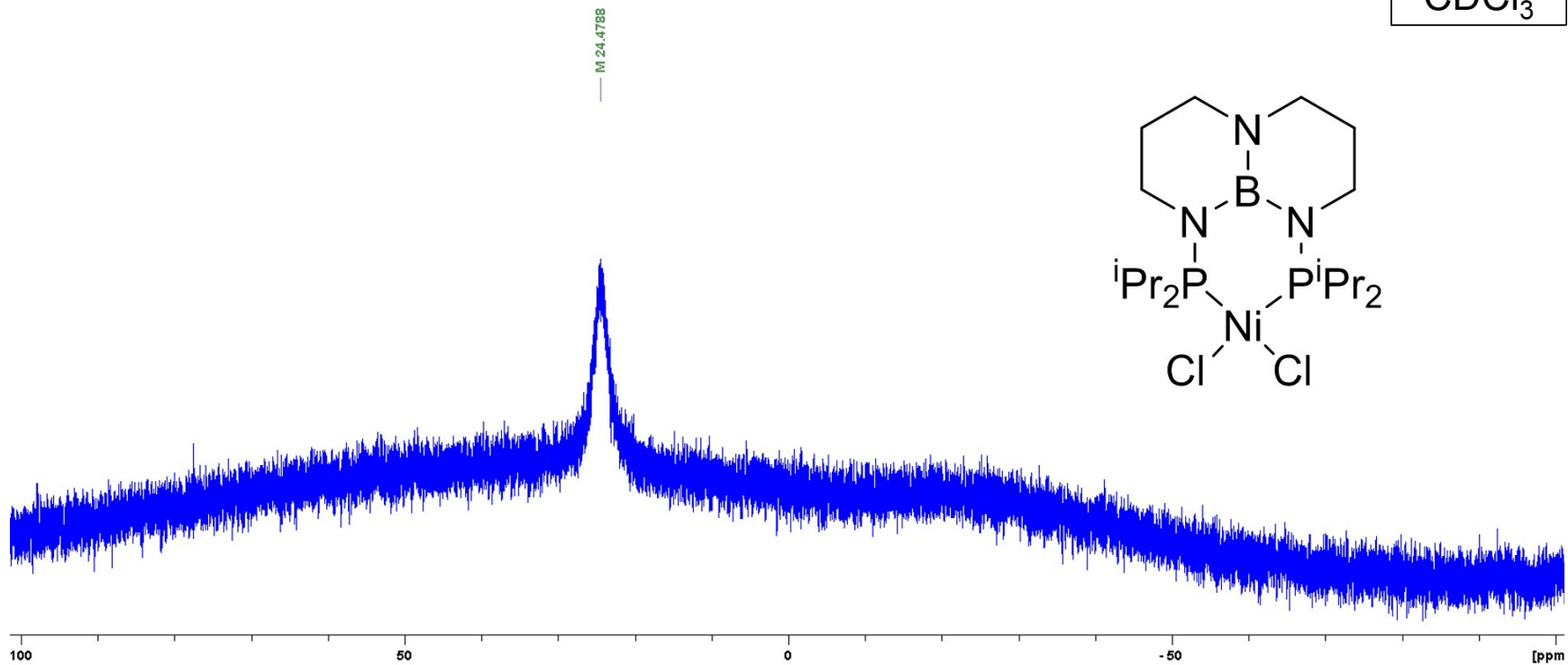


Figure S18. ¹¹B NMR spectrum of (*i*PrTBDPhos)NiCl₂ (**2**).

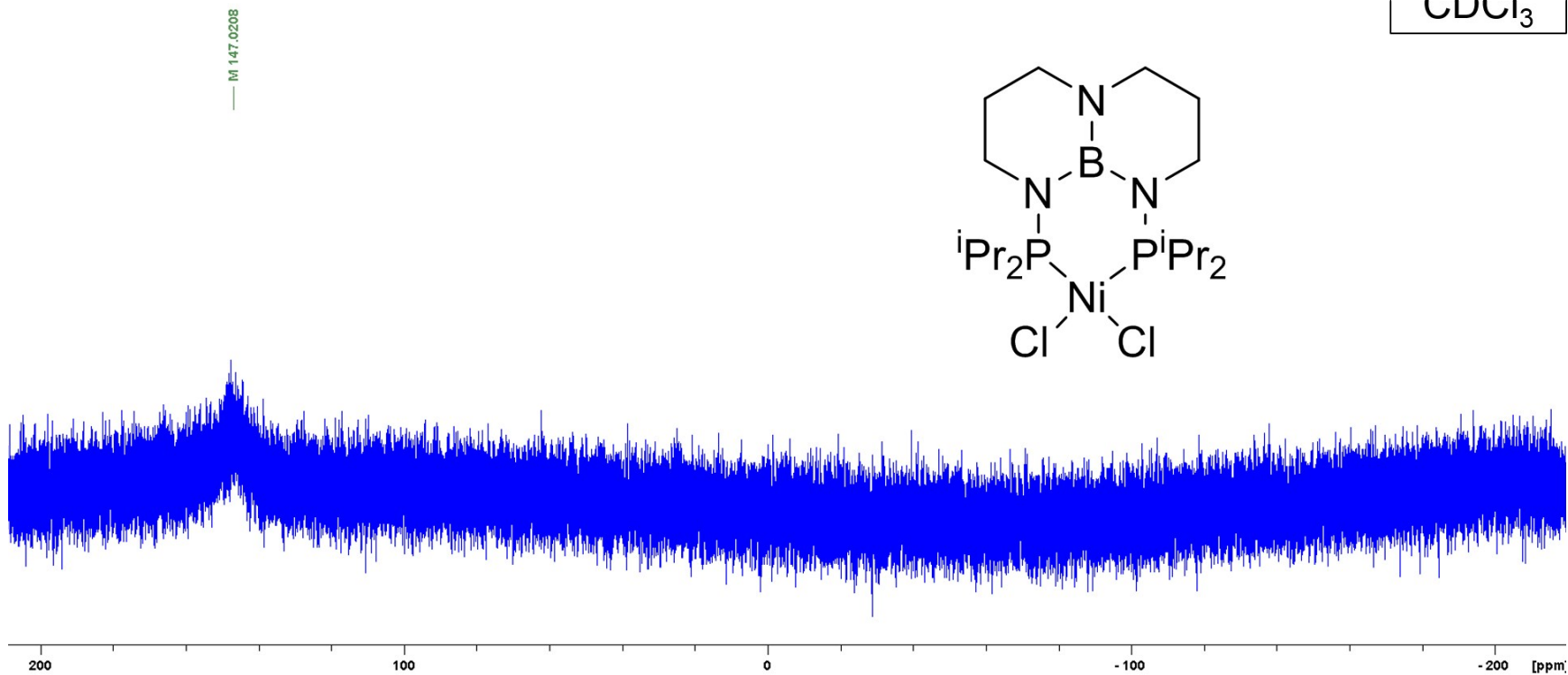


Figure S19. $^{31}\text{P}\{\text{H}\}$ NMR spectrum of $(\text{iPrTBDPhos})\text{NiCl}_2$ (**2**).

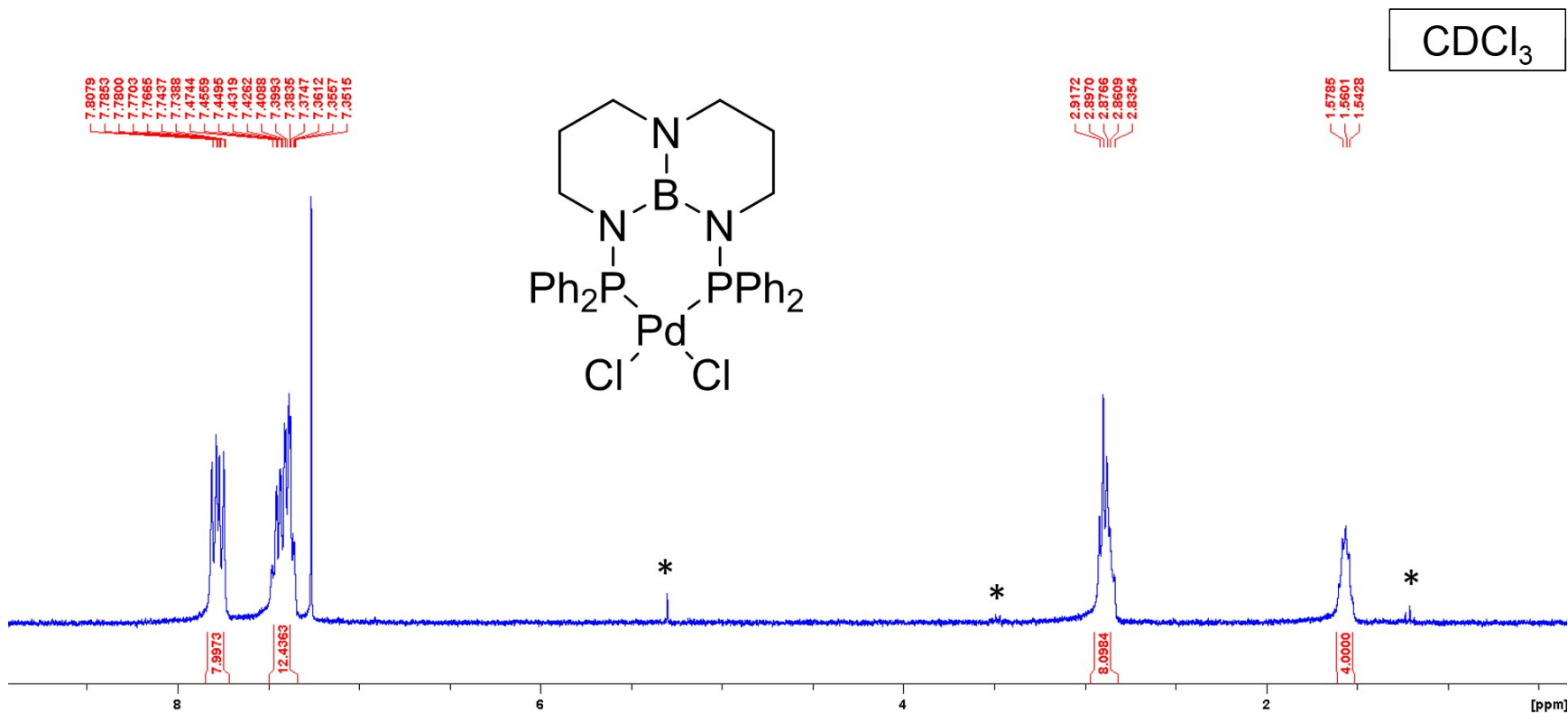


Figure S20. ¹H NMR spectrum of (^{Ph}TBDPhos)PdCl₂ (**3**). The * symbol indicates resonances assigned to residual CH₂Cl₂ and Et₂O solvent.

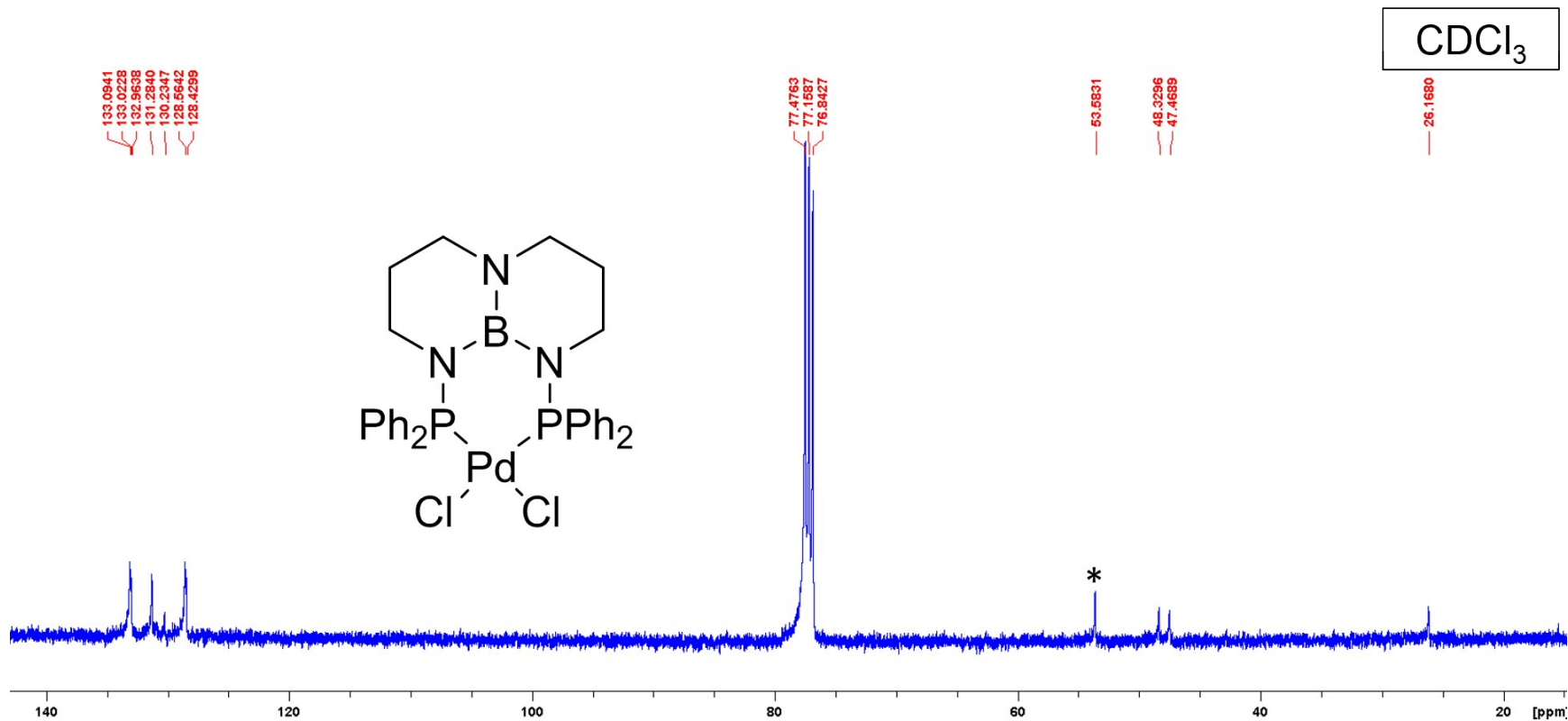


Figure S21. ^{13}C NMR spectrum of (^{Ph}TBDPhos)PdCl₂ (**3**). The * symbol indicates a resonances assigned to residual CH₂Cl₂.

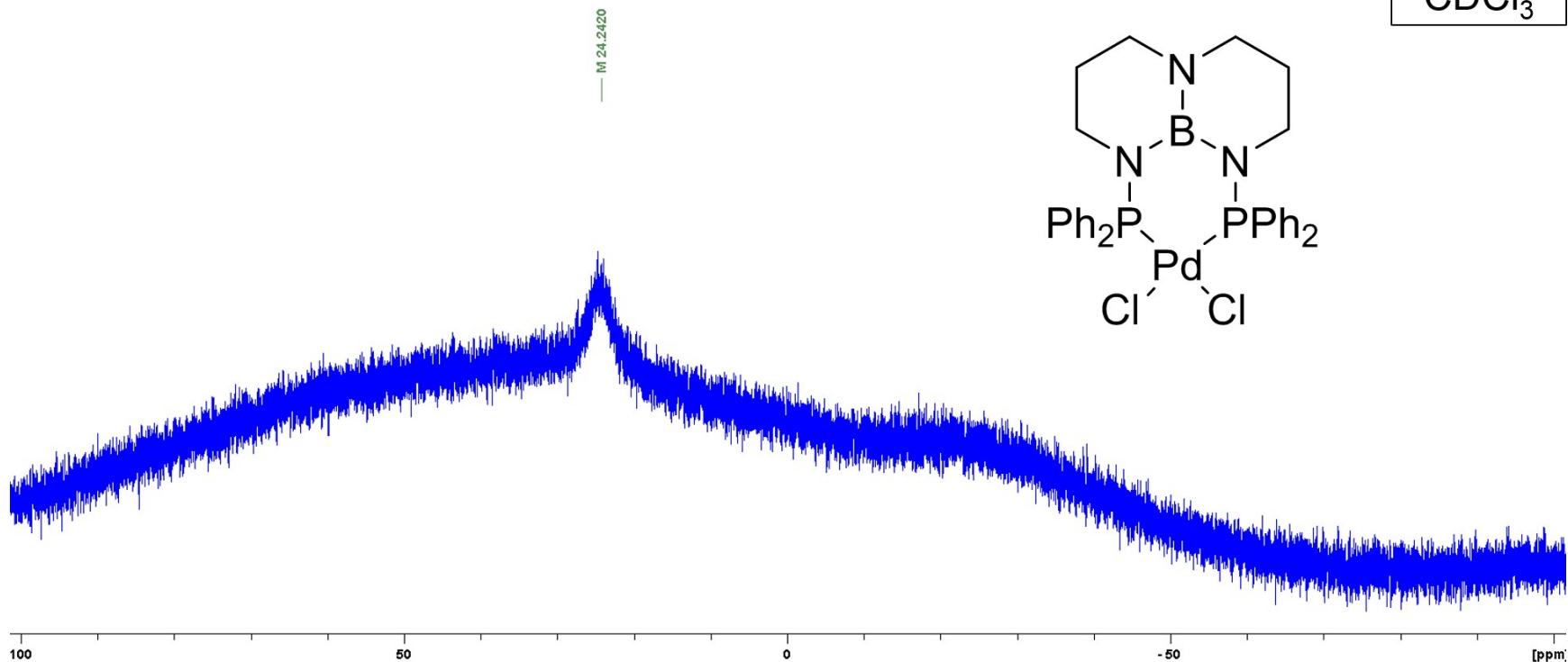


Figure S22. ¹¹B NMR spectrum of (^{Ph}TBDPhos)PdCl₂ (**3**).

CDCl_3

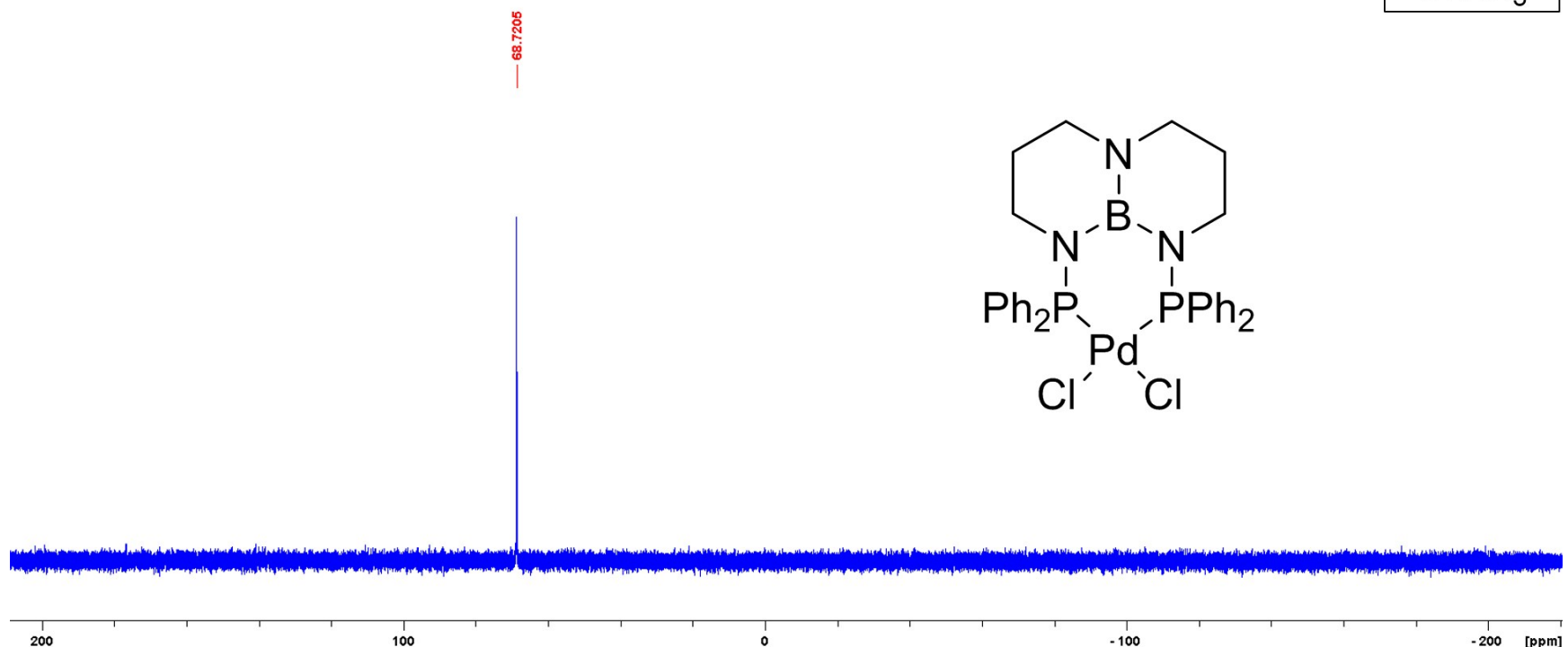


Figure S23. ${}^3\text{1}\text{P}\{{}^1\text{H}\}$ NMR spectrum of $({}^{\text{Ph}}\text{TBDPhos})\text{PdCl}_2$ (**3**).

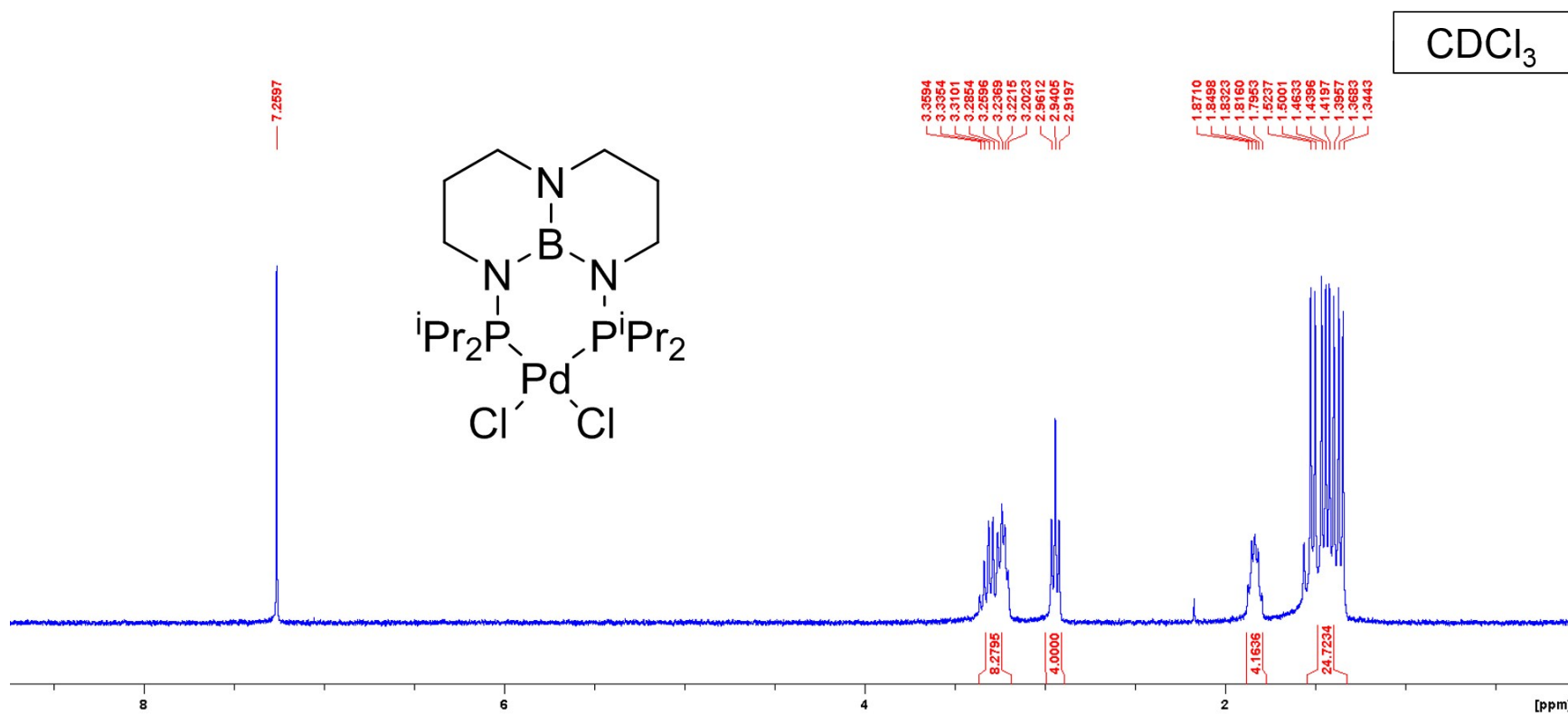


Figure S24. ¹H NMR spectrum of (ⁱPrTBDPhos)PdCl₂ (4).

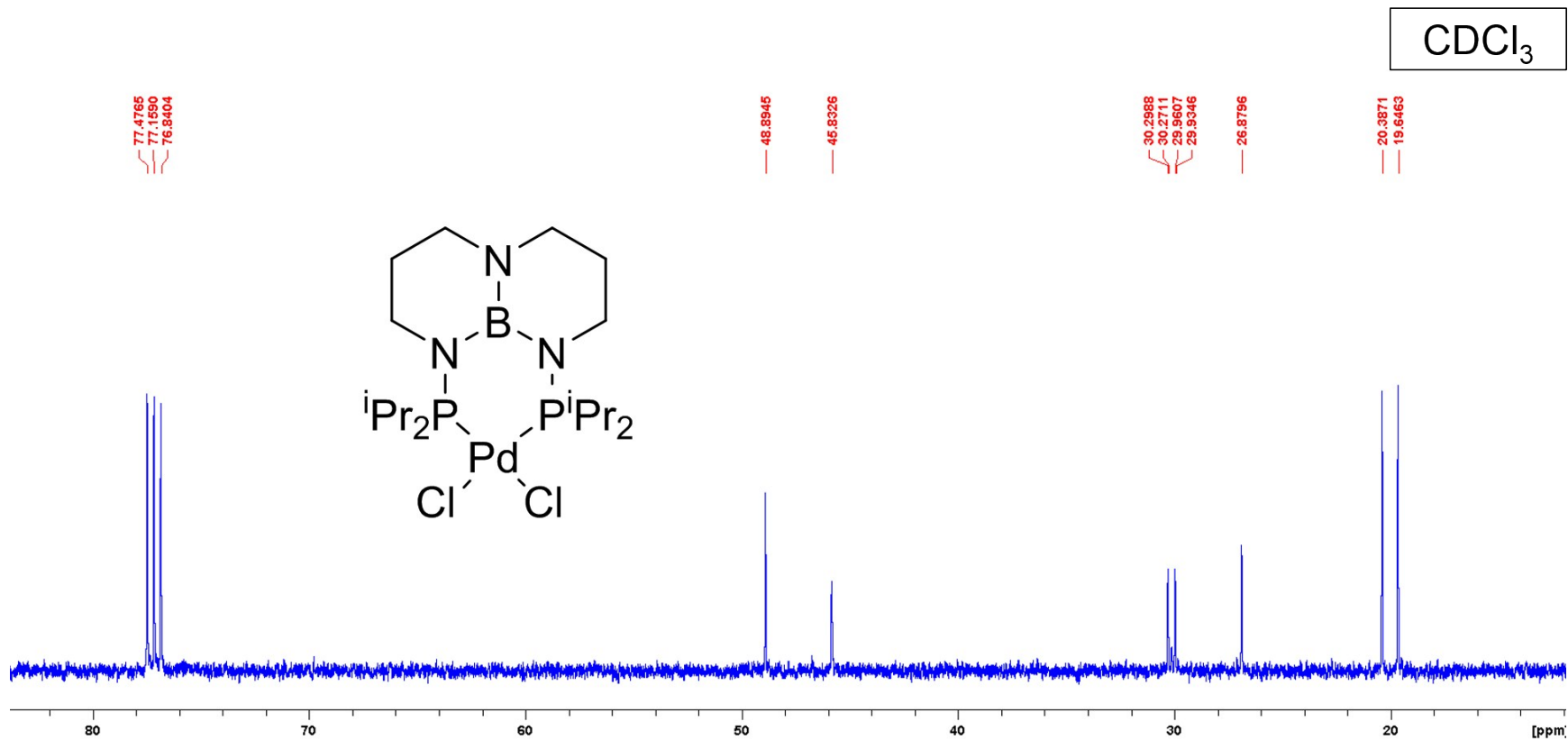


Figure S25. ¹³C NMR spectrum of (ⁱPrTBDPhos)PdCl₂ (**4**).

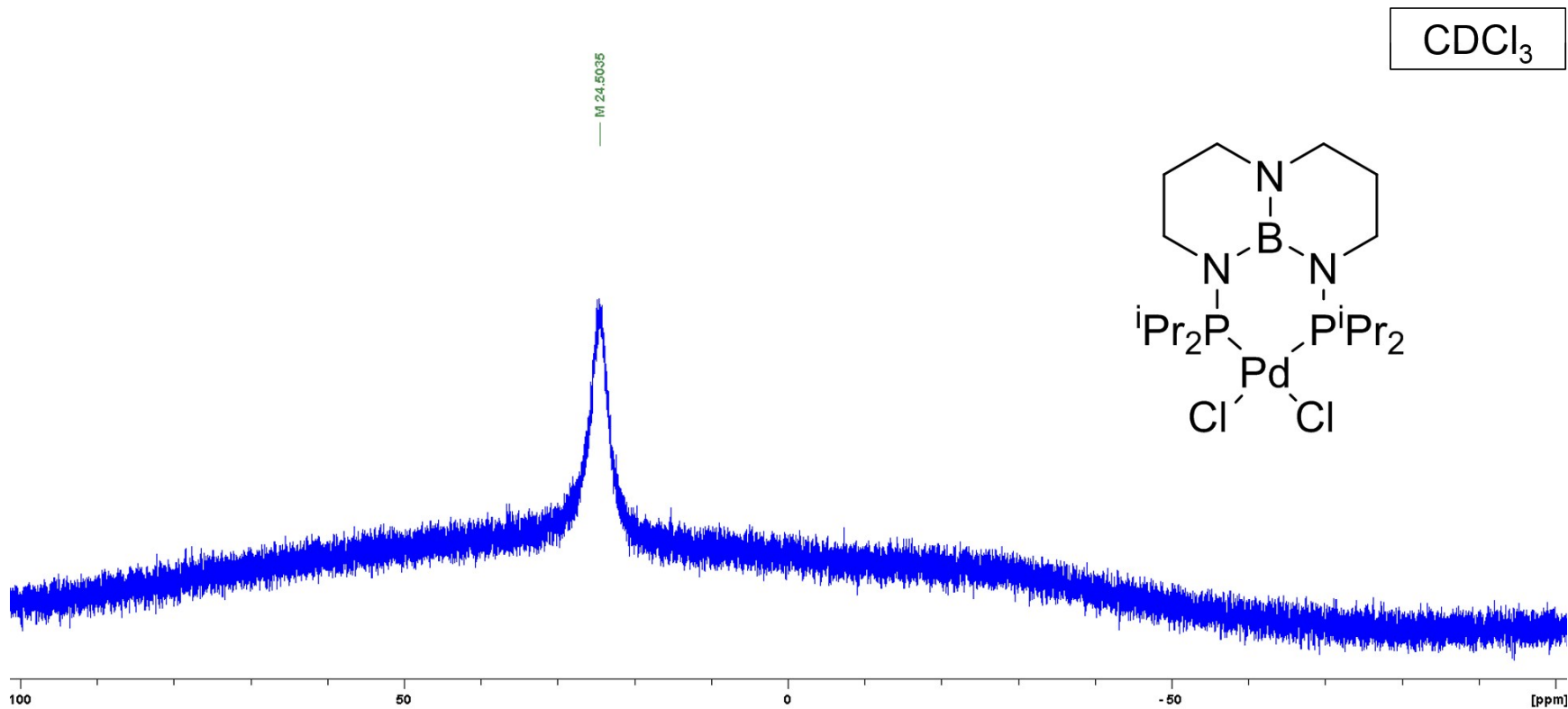


Figure S26. ¹¹B NMR spectrum of (ⁱPrTBDPhos)PdCl₂ (**4**).

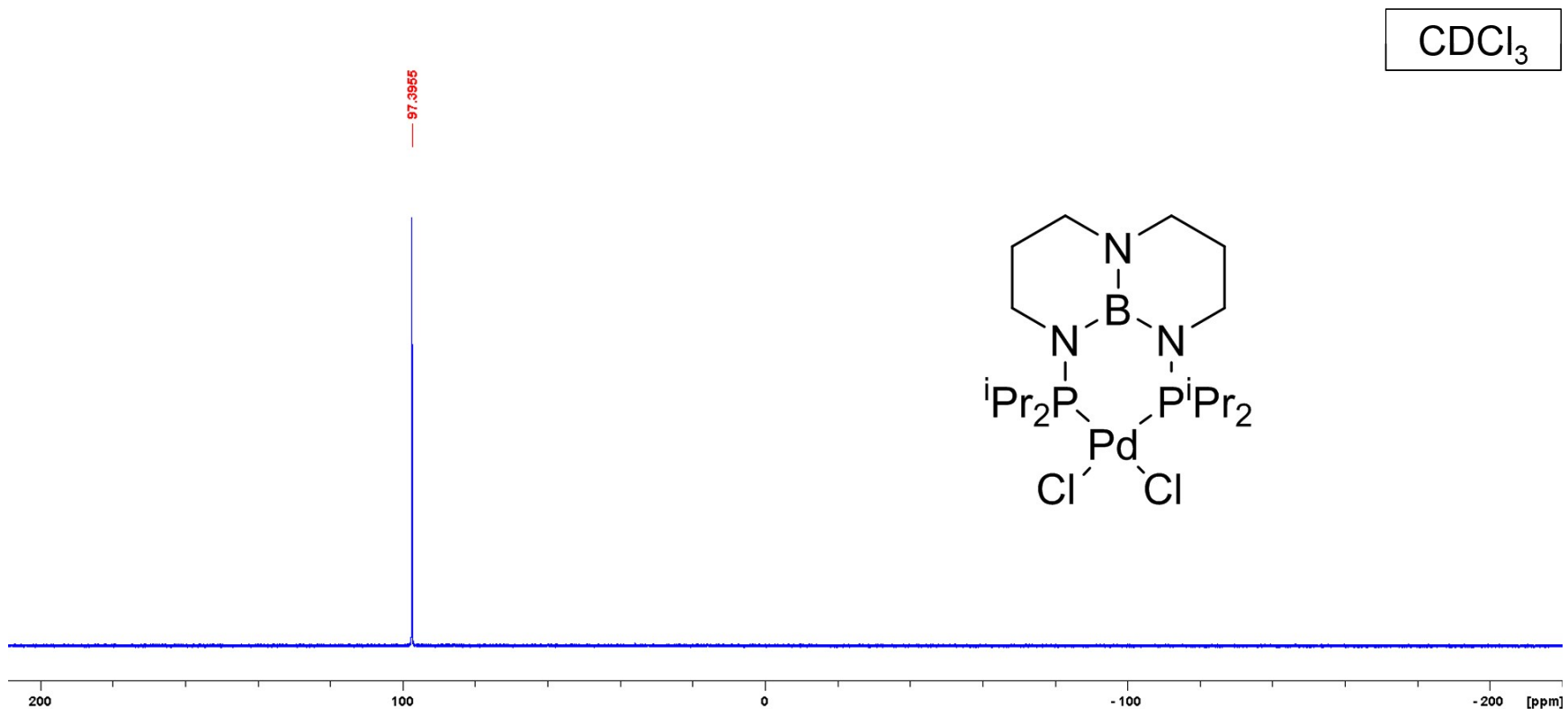


Figure S27. ${}^{31}\text{P}\{{}^1\text{H}\}$ NMR spectrum of $(\text{iPrTBDPhos})\text{PdCl}_2$ (**4**).

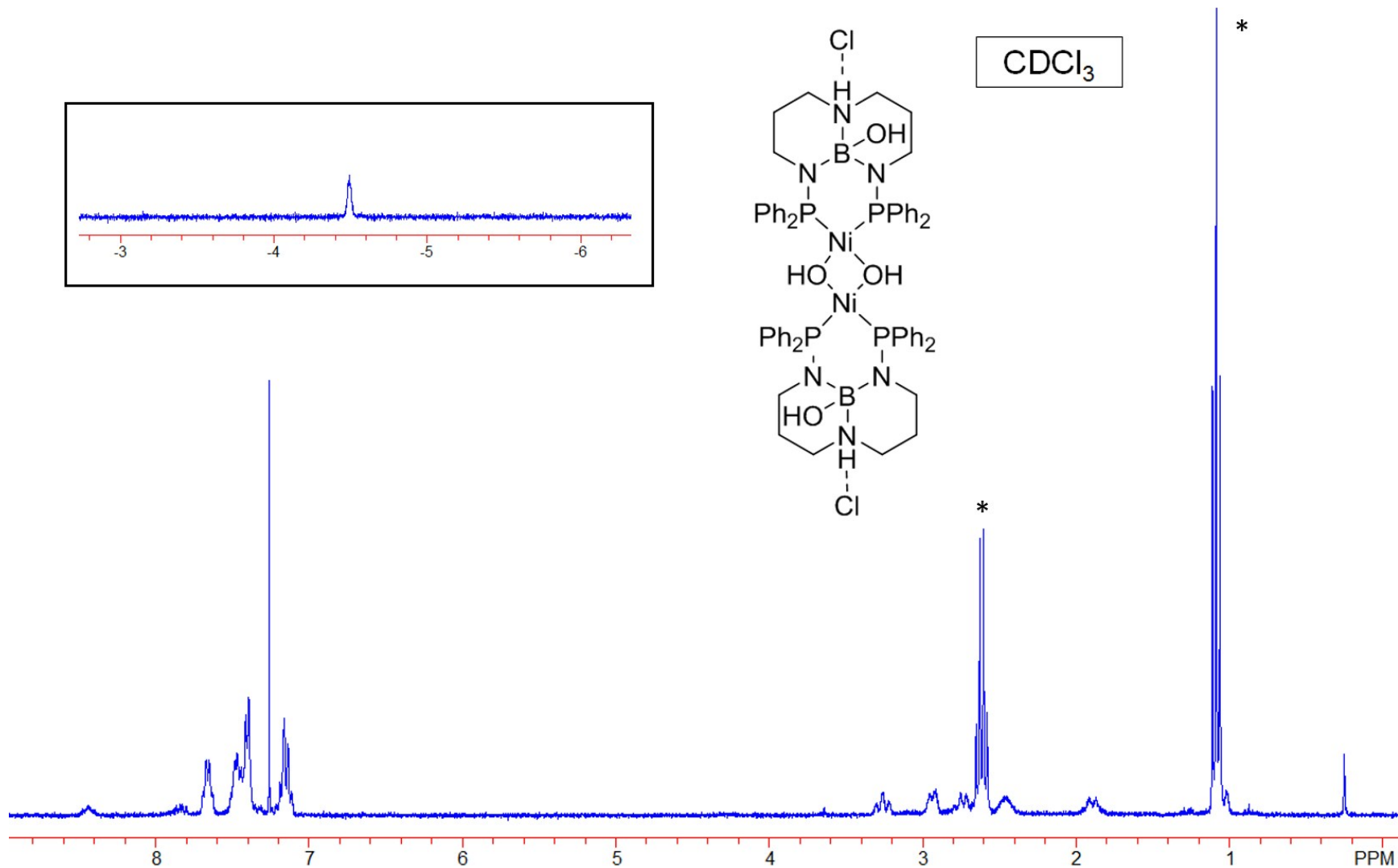


Figure S28. ^1H NMR spectrum of $\{[(^{\text{Ph}}\text{TBDPhos}-\text{H}_2\text{O})\text{Ni}]_2(\mu\text{-OH})_2\}\text{Cl}_2$ (**5**). The * symbol indicates resonances assigned to added NEt_3 . The inset shows the upfield shift assigned to the bridging hydroxide.

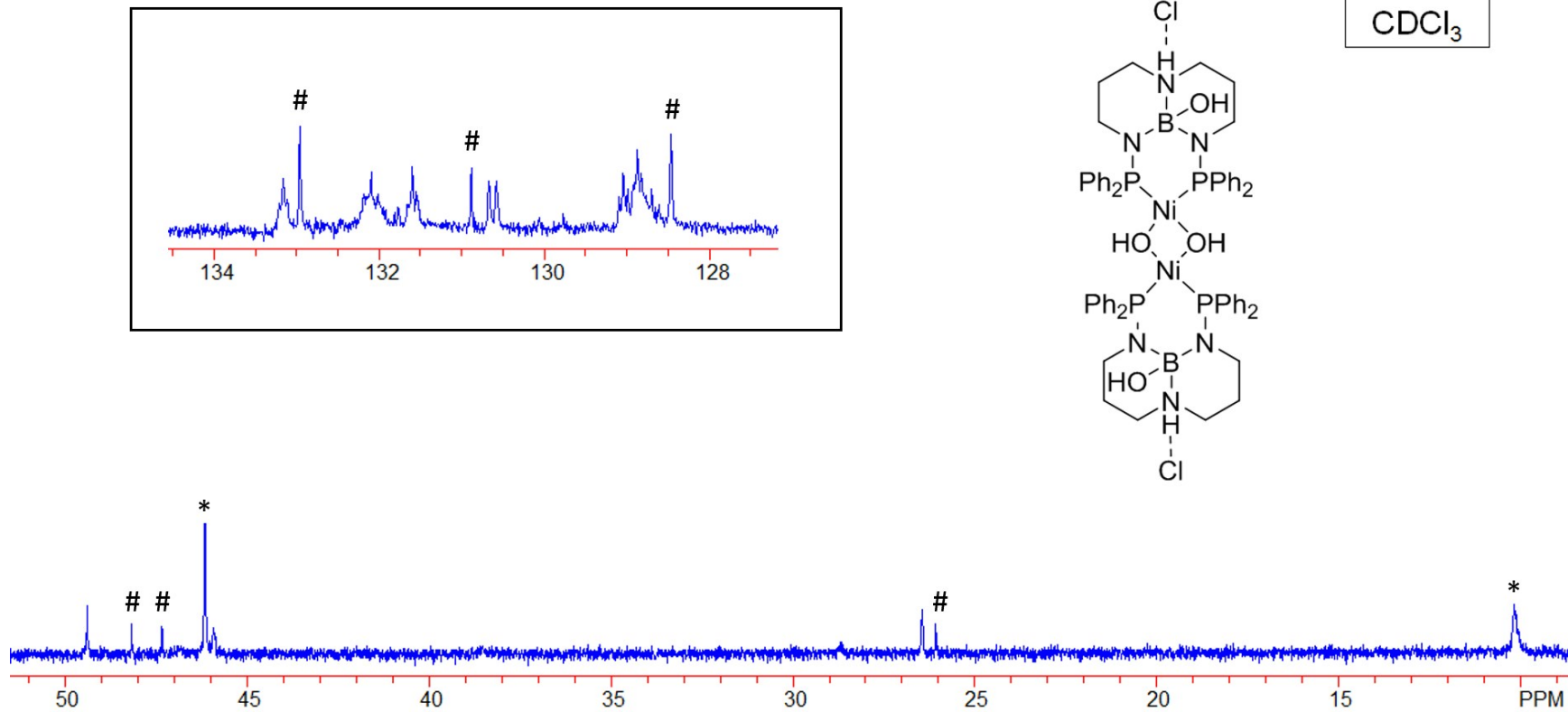


Figure S29. ^{13}C NMR spectrum of $\{[\text{PhTBDPhos}-\text{H}_2\text{O}]\text{Ni}\}_2(\mu\text{-OH})_2\text{Cl}_2$ (**5**). The * symbol indicates resonances assigned to added NEt_3 , and the # symbol indicates resonances assigned to **1**.

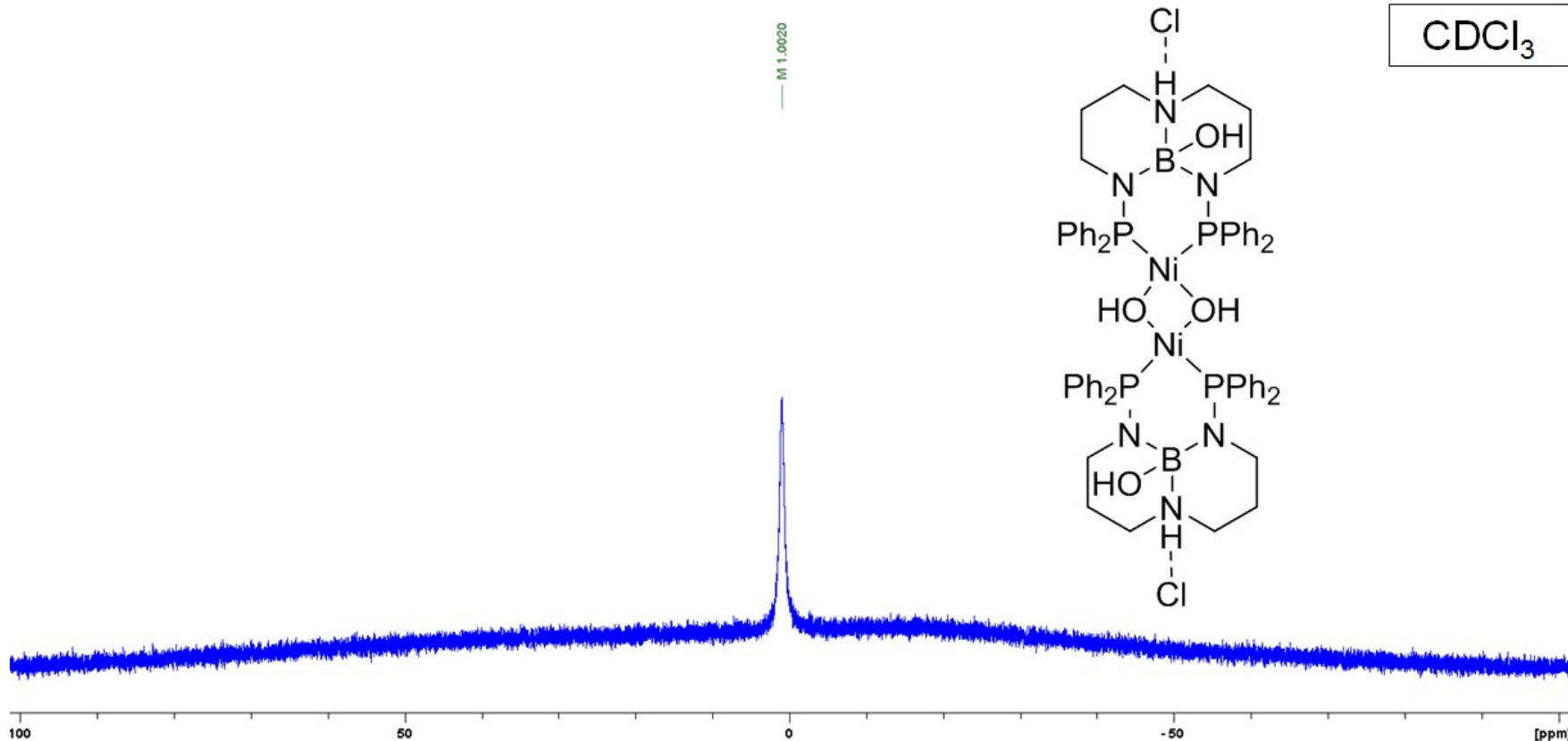


Figure S30. ^{11}B NMR spectrum of $\{[(^{\text{Ph}}\text{TBDPhos}-\text{H}_2\text{O})\text{Ni}]_2(\mu-\text{OH})_2\}\text{Cl}_2$ (**5**) taken before overnight ^{13}C NMR data collection.

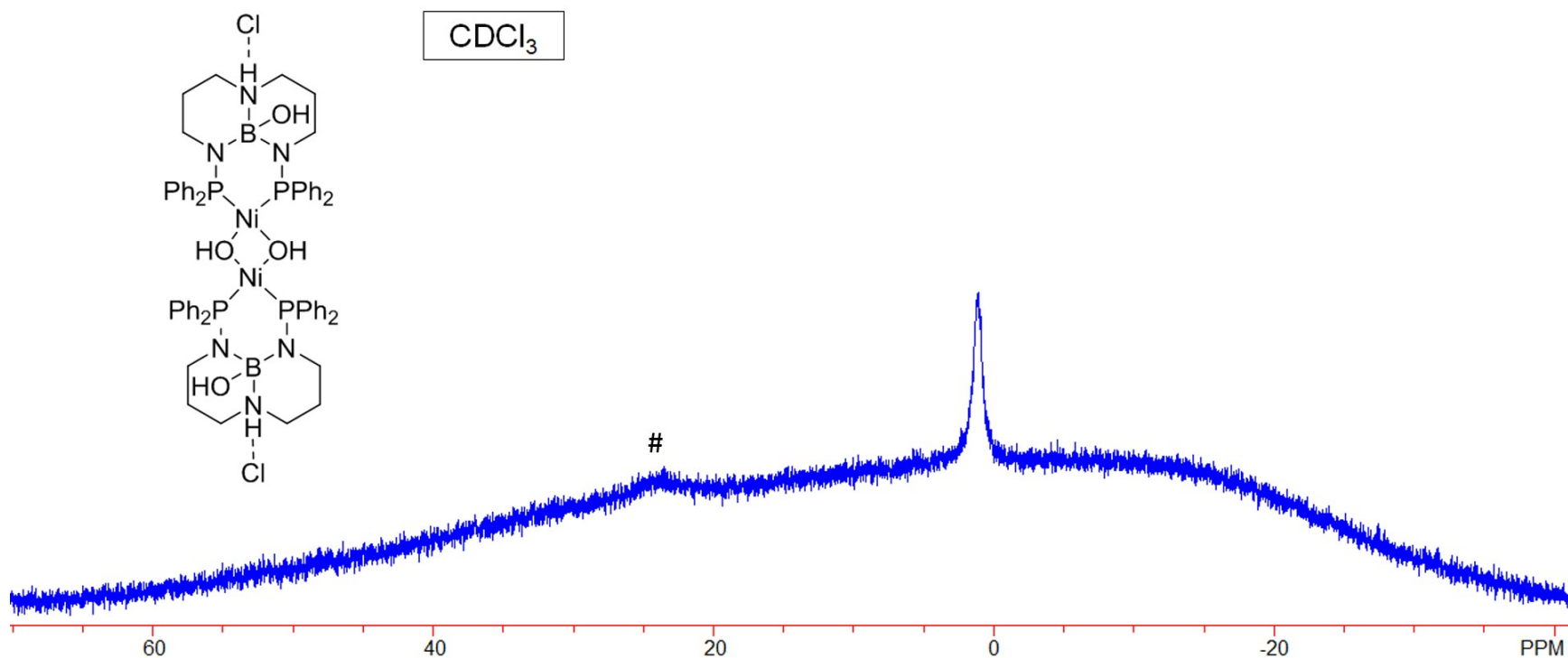


Figure S31. ^{11}B NMR spectrum of $\{[(^{\text{Ph}}\text{TBDPhos}-\text{H}_2\text{O})\text{Ni}]_2(\mu\text{-OH})_2\}\text{Cl}_2$ (**5**) taken after overnight ^{13}C NMR data collection. The # symbol indicates the broad resonance assigned to **1**.

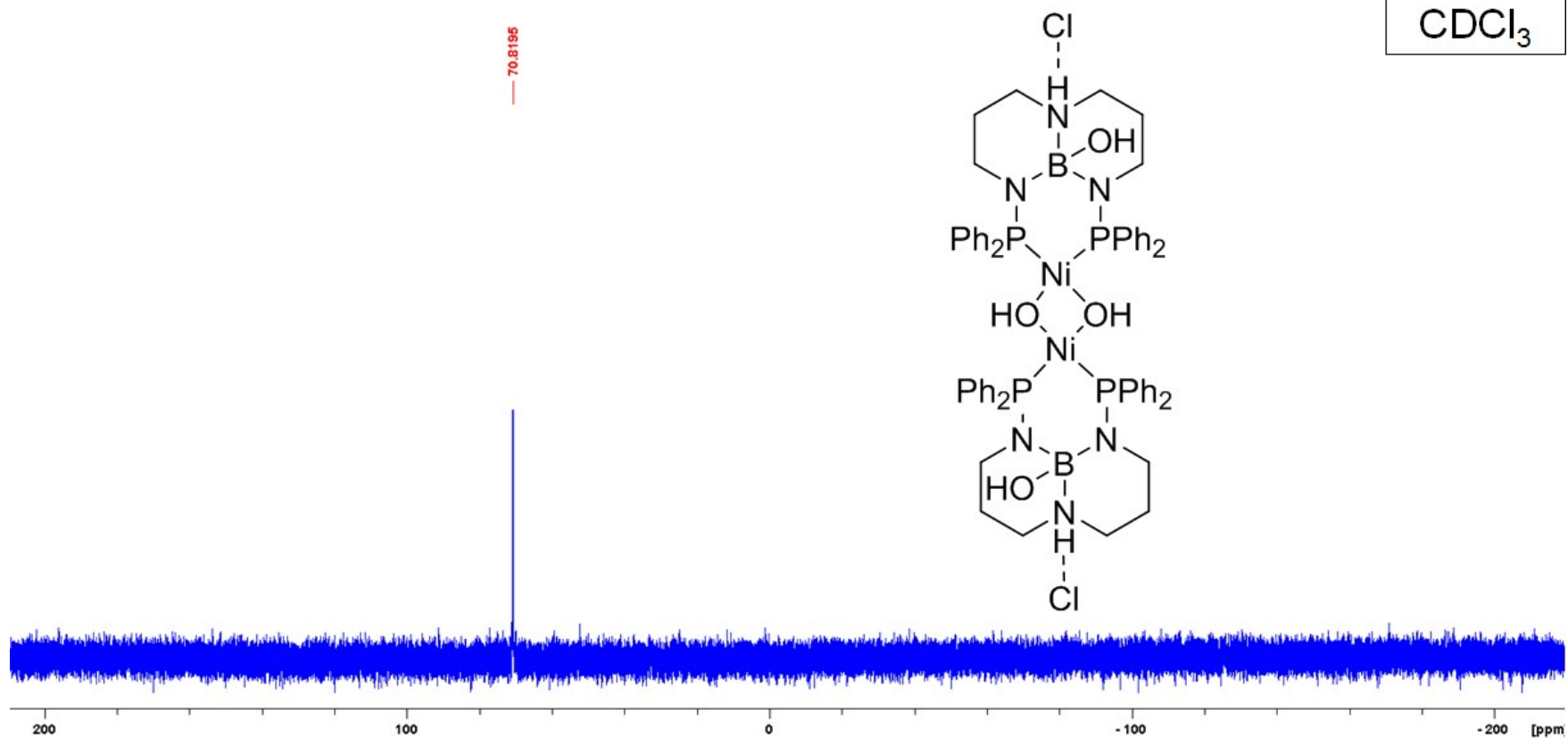


Figure S32. $^{31}\text{P}\{\text{H}\}$ NMR spectrum of $\{[(^{\text{Ph}}\text{TBDPhos}-\text{H}_2\text{O})\text{Ni}]_2(\mu-\text{OH})_2\}\text{Cl}_2$ (**5**).

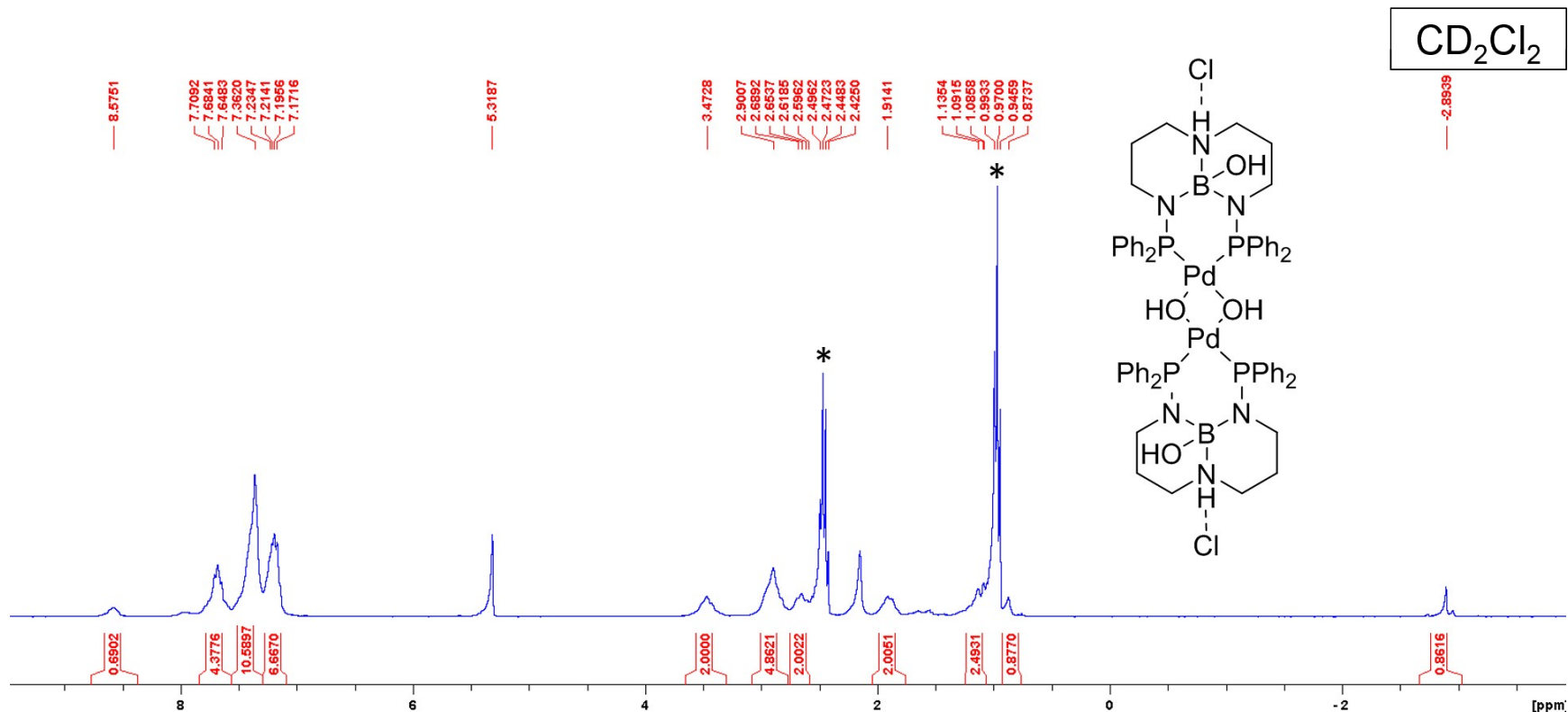


Figure S33. ¹H NMR spectrum of $\{[(\text{PhTBDPhos}-\text{H}_2\text{O})\text{Pd}]_2(\mu\text{-OH})_2\}\text{Cl}_2$ (**6**). The * symbol indicates resonances assigned to added NEt₃.

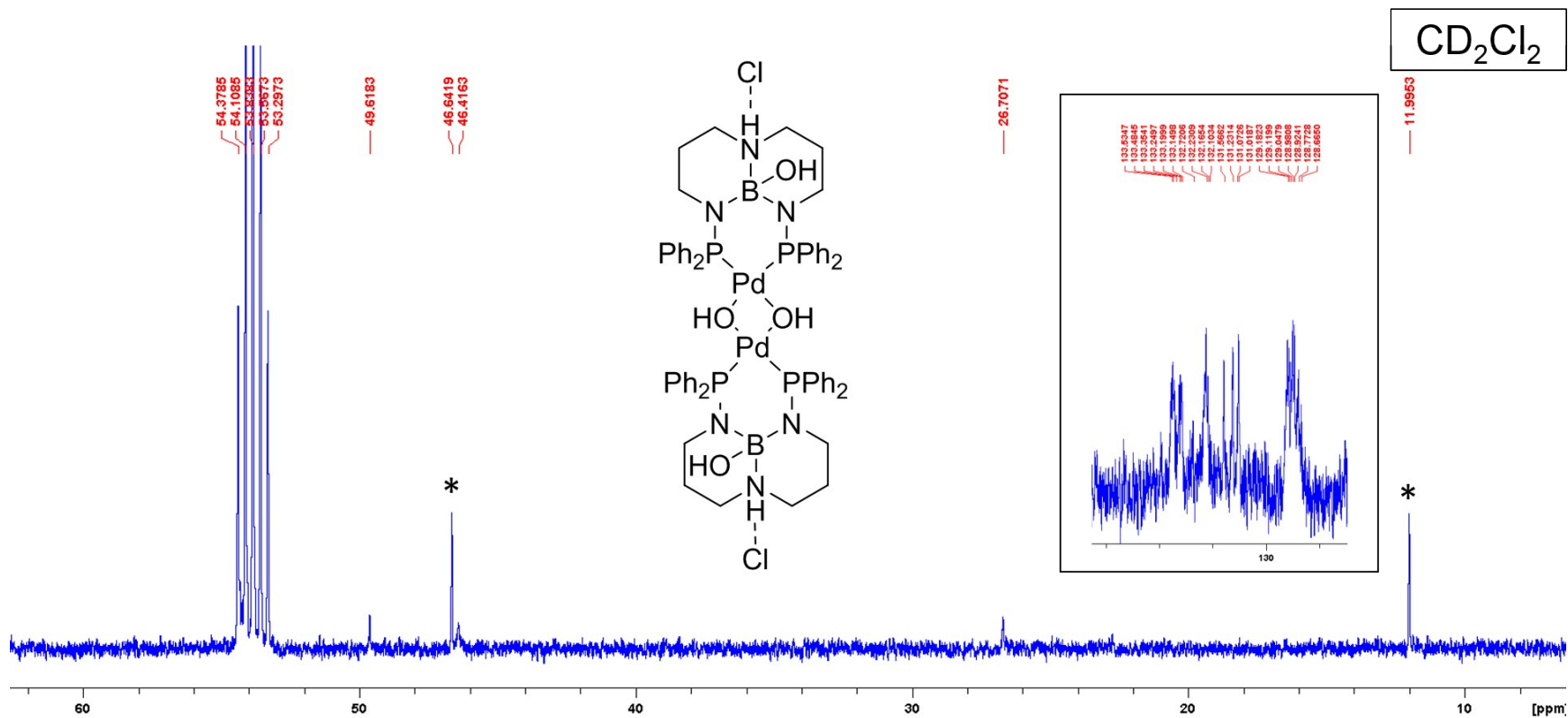


Figure S34. ^{13}C NMR spectrum of $\{[({}^{\text{Ph}}\text{TBDPhos}-\text{H}_2\text{O})\text{Pd}]_2(\mu-\text{OH})_2\}\text{Cl}_2$ (**6**). The * symbol indicates resonances assigned to added NEt_3 .

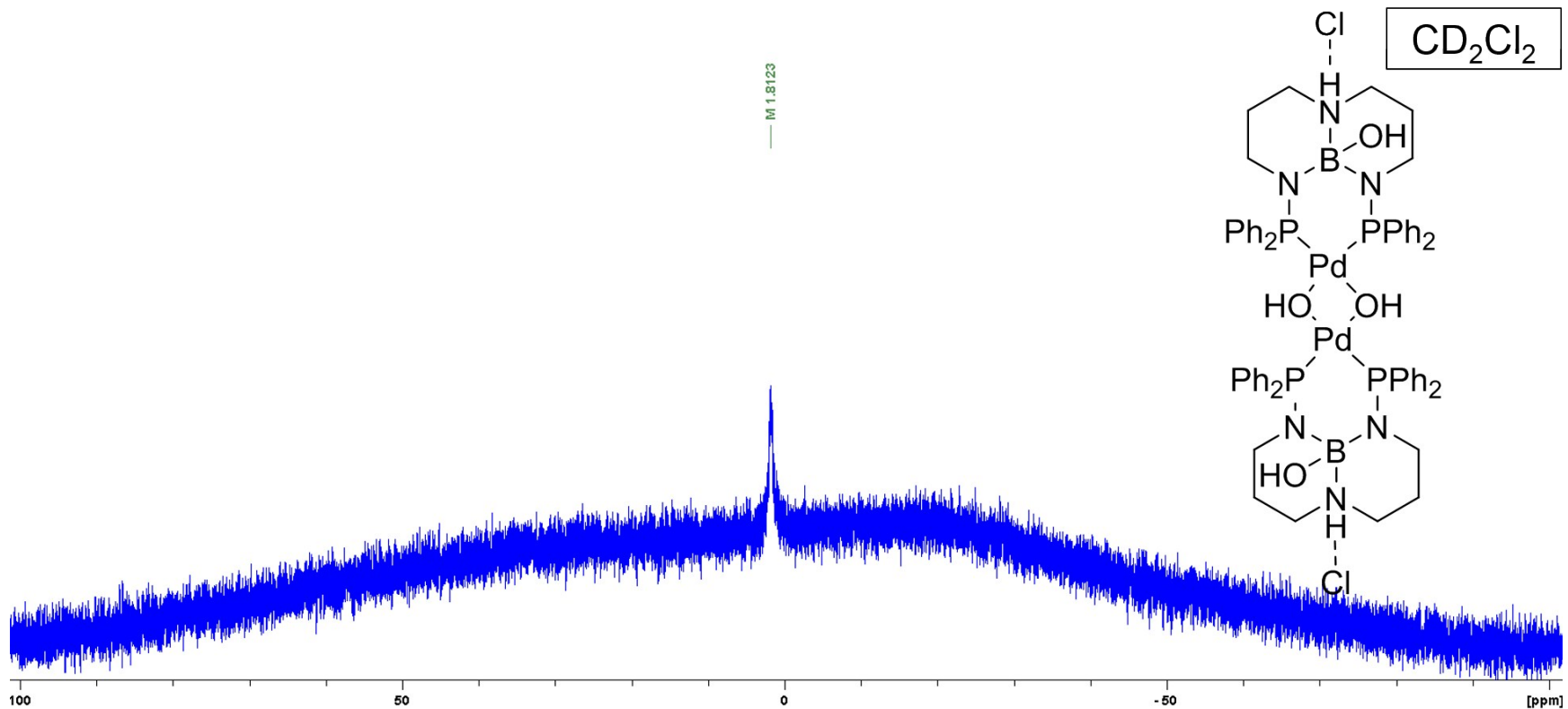


Figure S35. ^{11}B NMR spectrum of $\{[({}^{\text{Ph}}\text{TBDPhos}-\text{H}_2\text{O})\text{Pd}]_2(\mu-\text{OH})_2\}\text{Cl}_2$ (**6**).

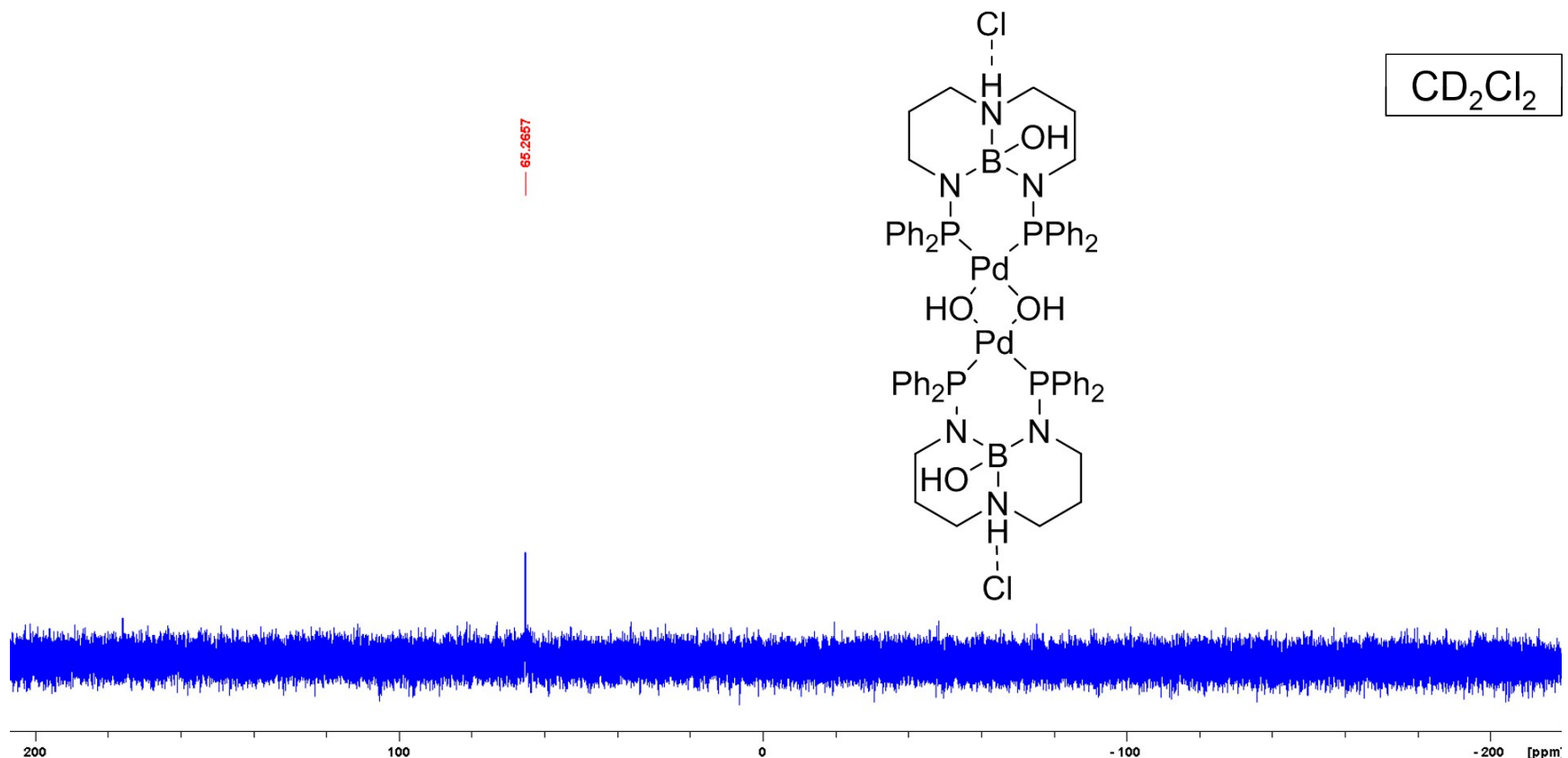


Figure S36. $^{31}\text{P}\{\text{H}\}$ NMR spectrum of $\{[(\text{PhTBDPhos}-\text{H}_2\text{O})\text{Pd}]_2(\mu\text{-OH})_2\}\text{Cl}_2$ (**6**).

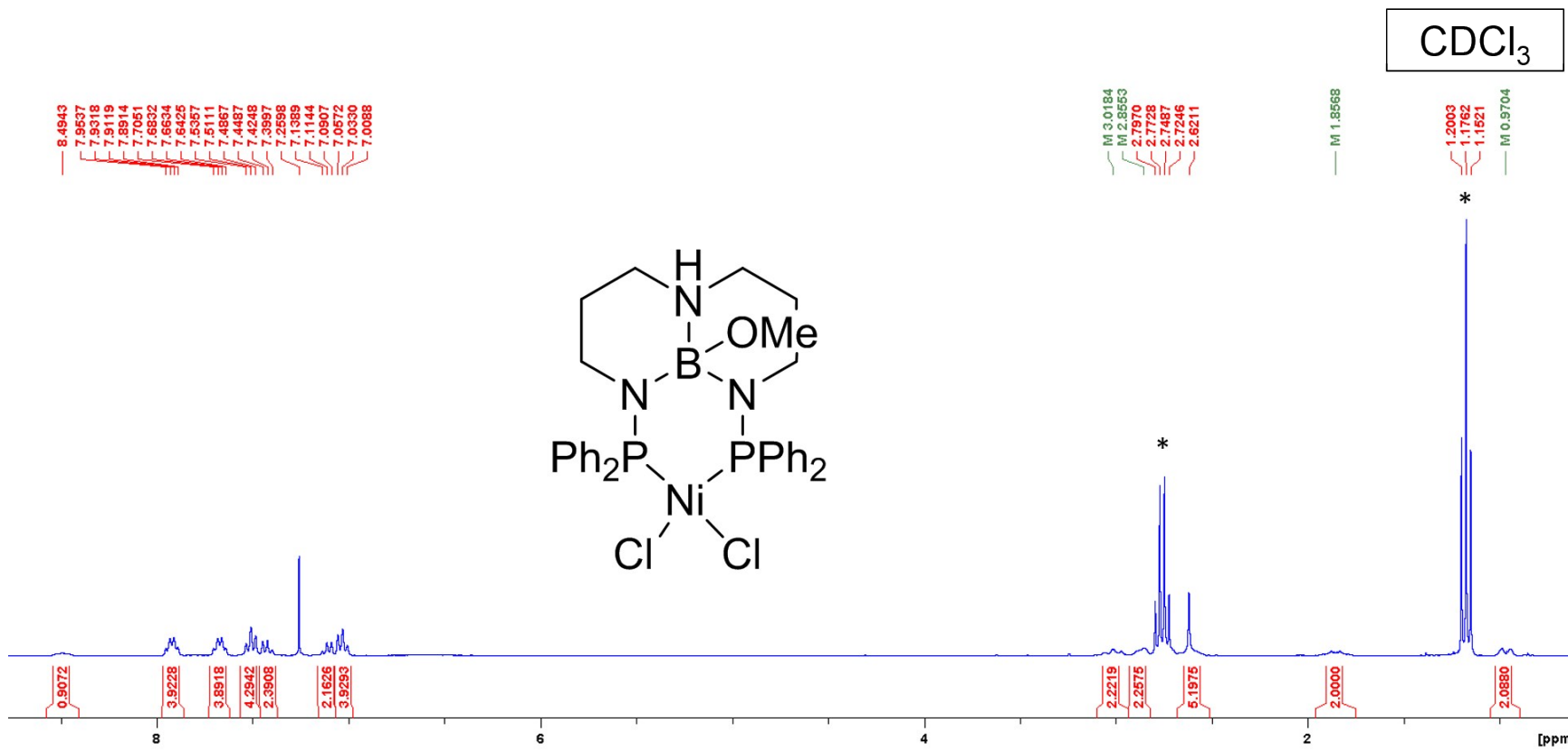


Figure S37. ¹H NMR spectrum of (^{Ph}TBDPhos-MeOH)NiCl₂ (**7**). The * symbol indicates resonances assigned to added NEt₃.

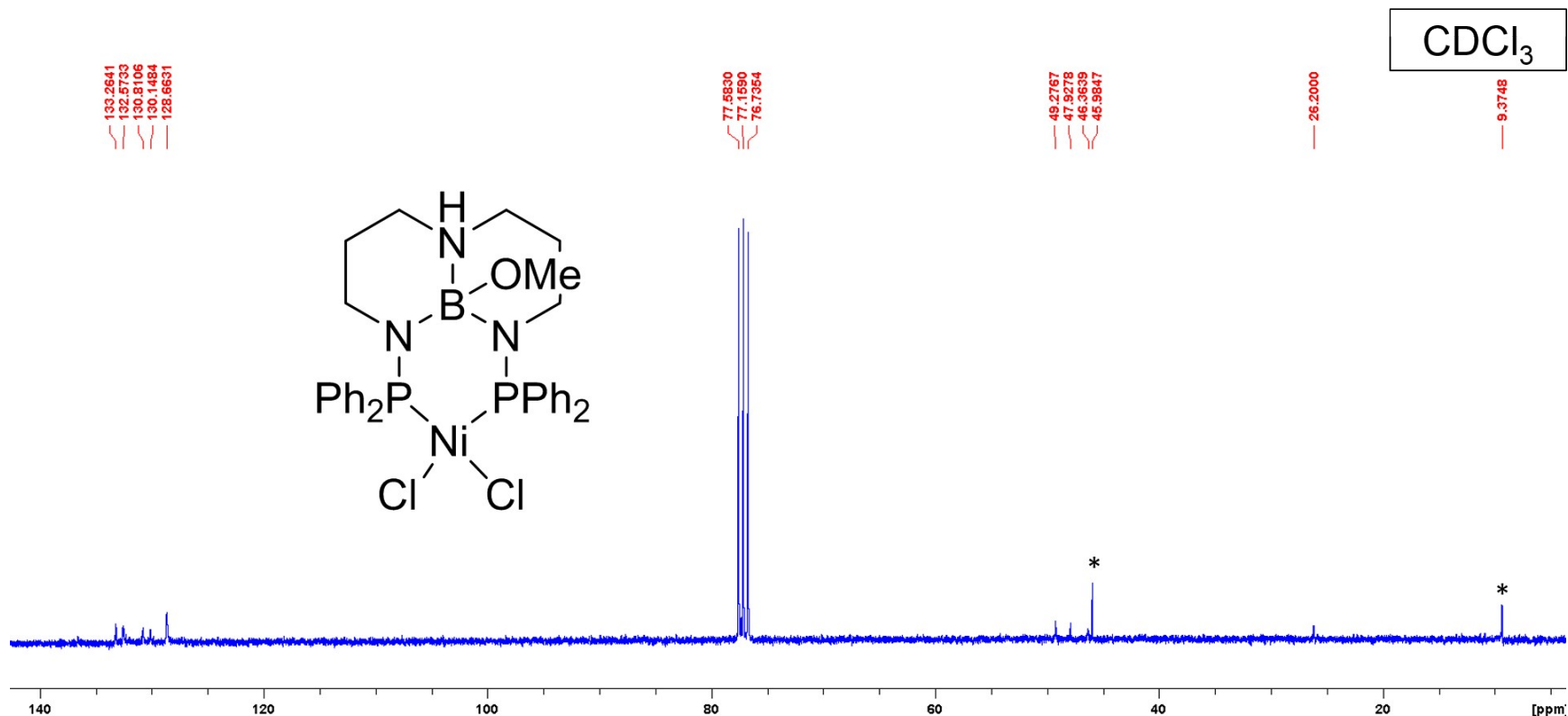


Figure S38. ¹³C NMR spectrum of (^{Ph}TBDPhos-MeOH)NiCl₂ (7). The * symbol indicates resonances assigned to added NEt₃.

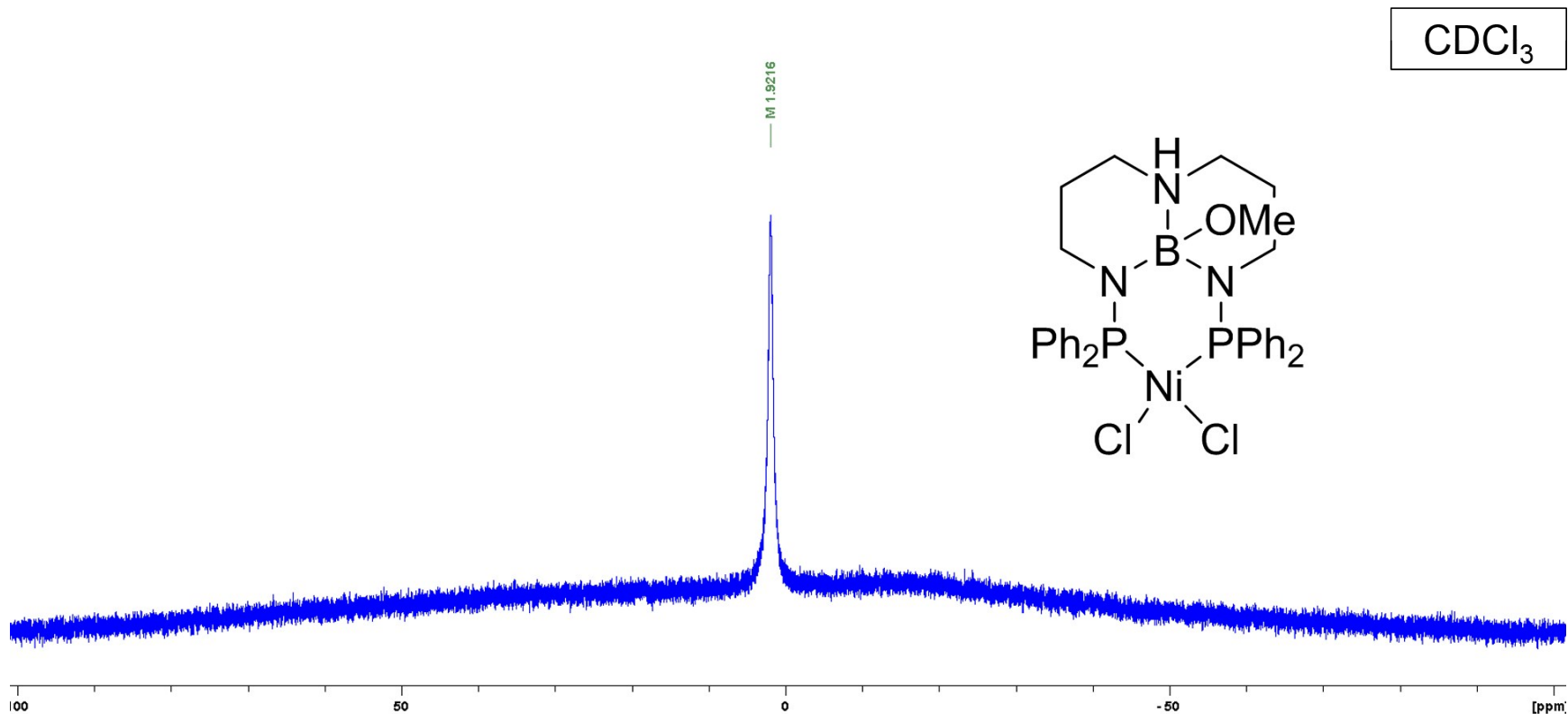


Figure S39. ¹¹B NMR spectrum of (^{Ph}TBDPhos-MeOH)NiCl₂ (7).

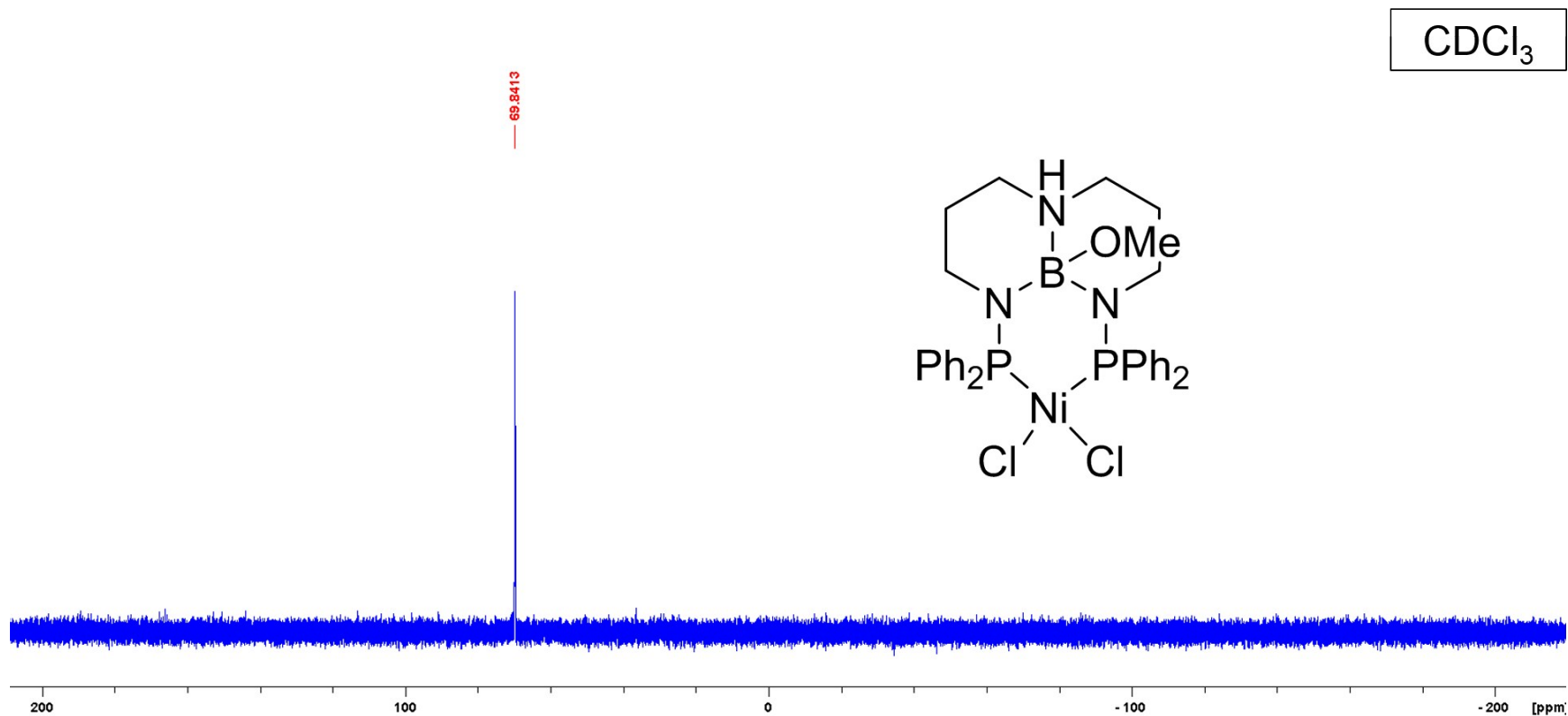
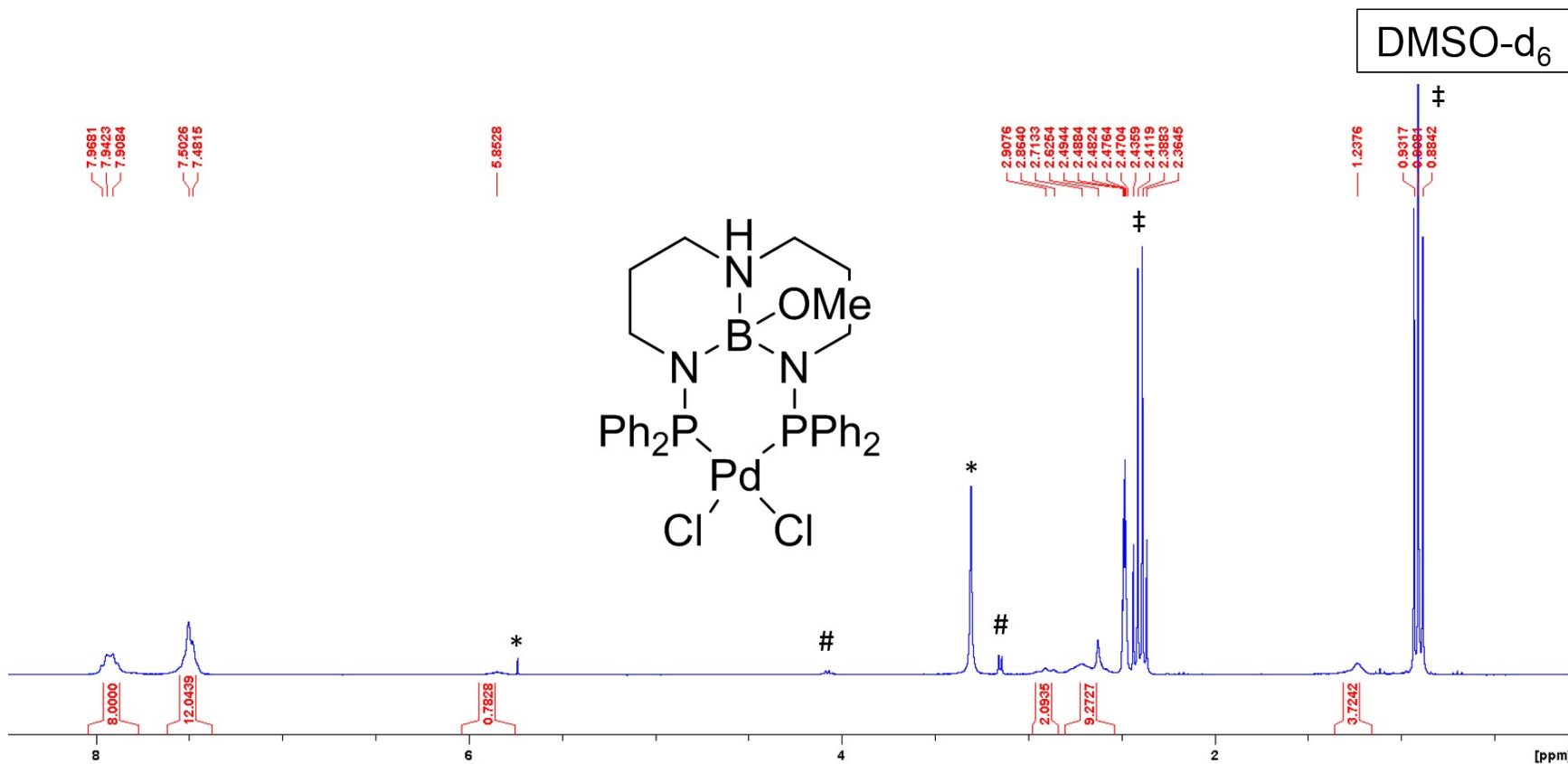


Figure S40. $^{31}\text{P}\{^1\text{H}\}$ NMR spectrum of $(^{\text{Ph}}\text{TBDPhos}-\text{MeOH})\text{NiCl}_2$ (**7**).



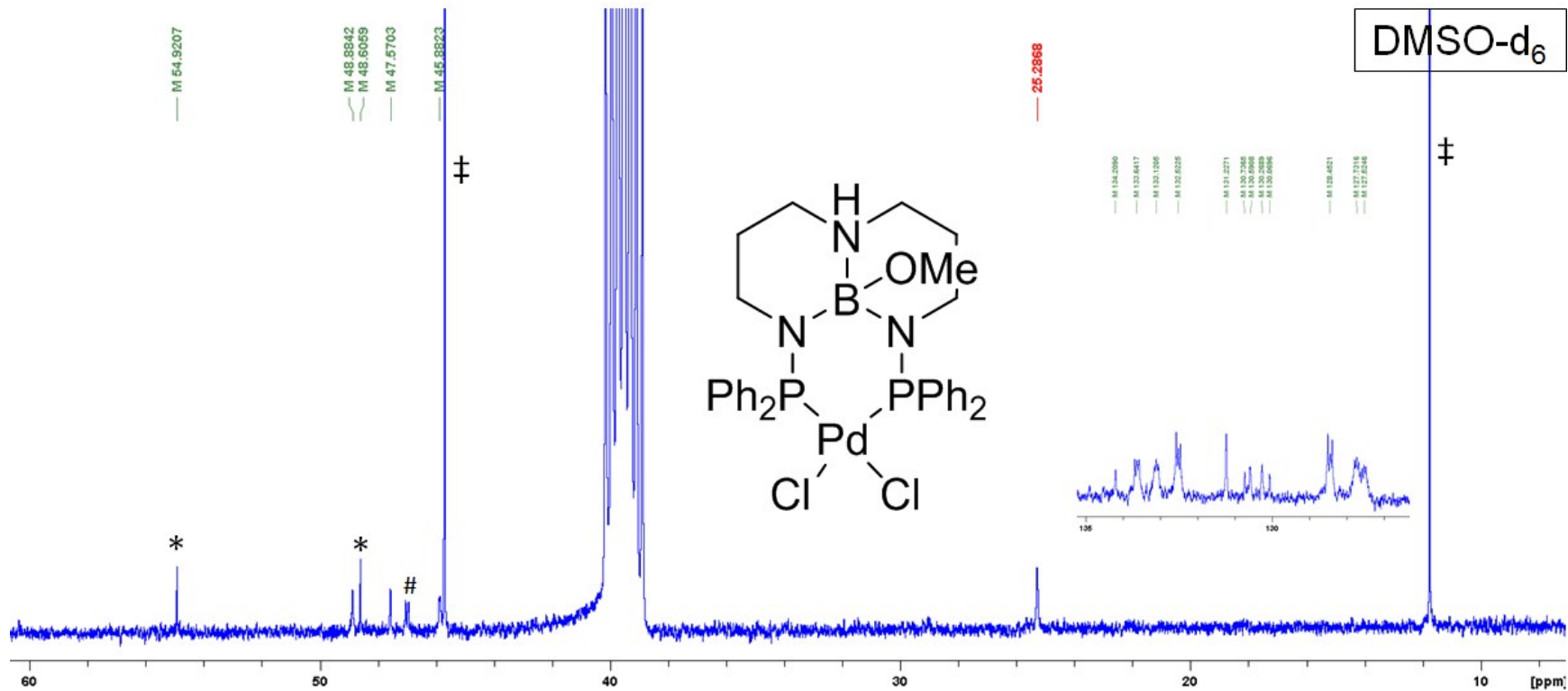


Figure S42. ^{13}C NMR spectrum of ($^{\text{Ph}}\text{TBDPhos}$ -MeOH) PdCl_2 (**8**). The * symbol indicates resonances assigned to CH_2Cl_2 and free MeOH. The # symbol indicates unassigned peak which had been growing during overnight data collection. The ‡ symbol indicates resonances assigned to added NEt_3 .

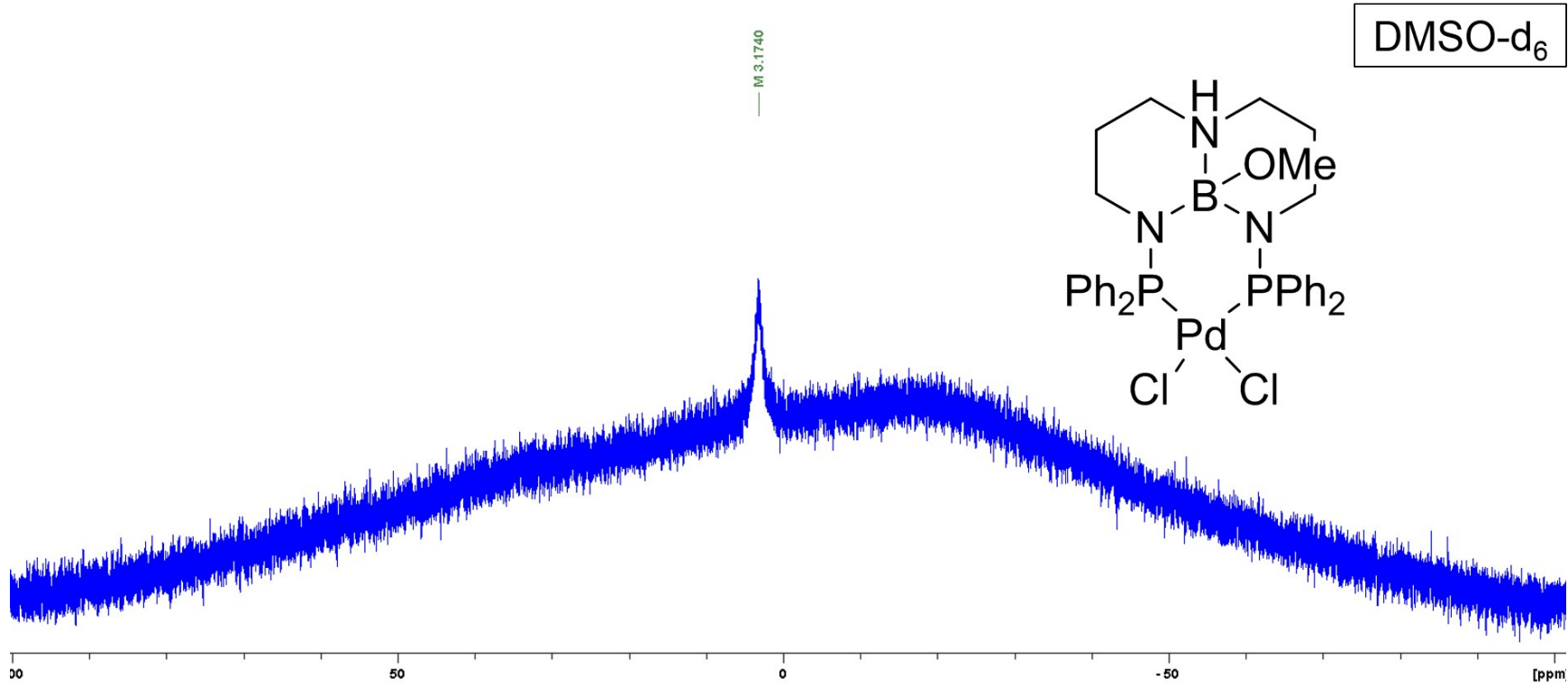


Figure S43. ¹¹B NMR spectrum of (^{Ph}TBDPhos-MeOH)PdCl₂ (8).

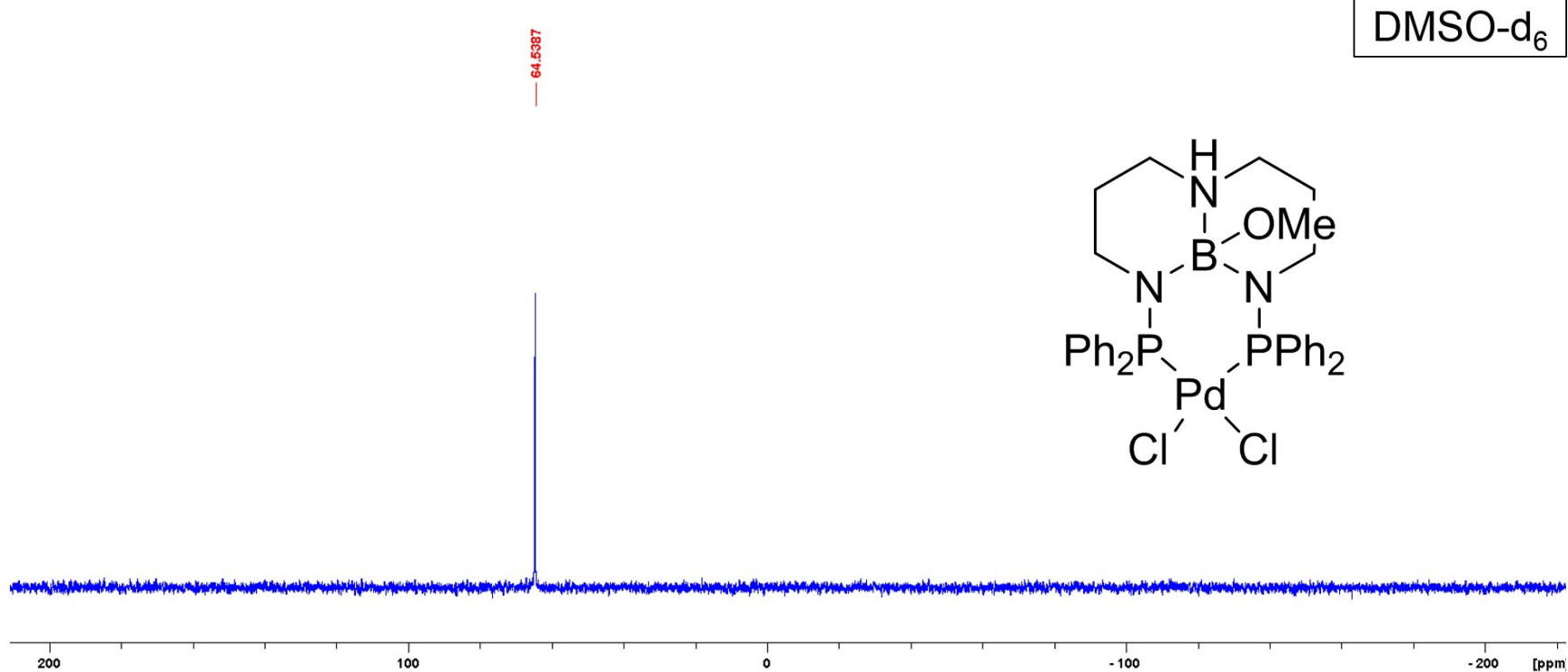


Figure S44. $^{31}\text{P}\{\text{H}\}$ NMR spectrum of (^{Ph}TBDPhos-MeOH)PdCl₂ (**8**).

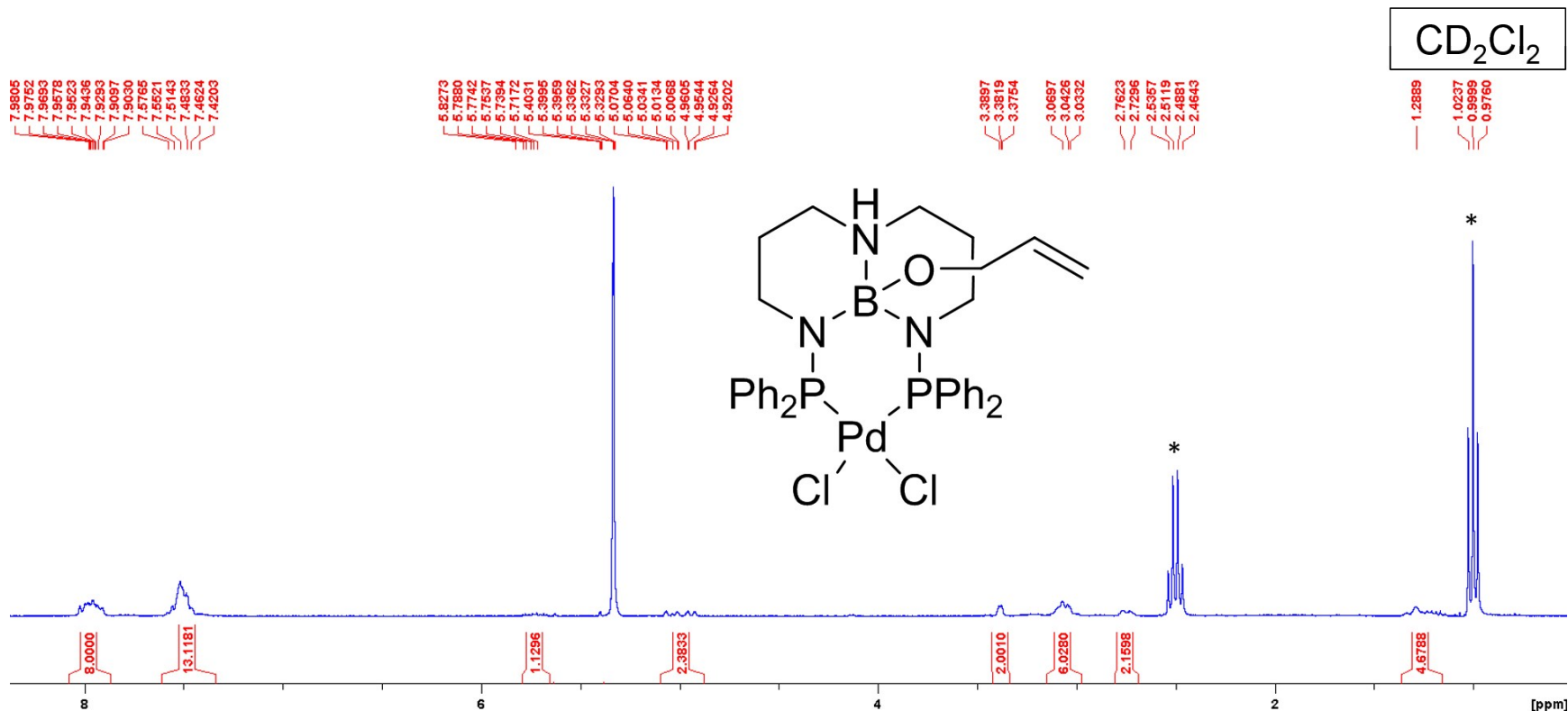
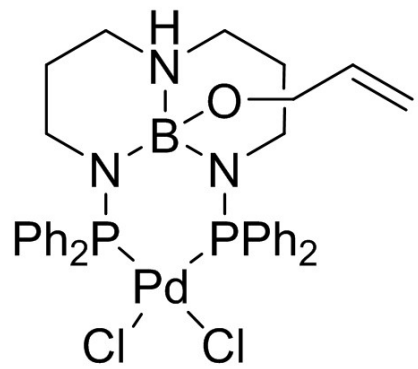


Figure S45. ^1H NMR spectrum of ($^{\text{Ph}}\text{TBDPhos}$ -C₃H₅OH)PdCl₂ (**9**). The * symbol indicates resonances assigned to added NEt₃.

134.9269
134.3350
134.2764
134.2180
134.2142
133.3742
133.3173
133.2585
133.1998
133.1357
131.6111
131.3427
130.9887
128.8087
128.6538
128.5763
128.5212
128.4697
128.4133
128.3559

112.8422



60.8544

50.2667
46.6526
46.4492

26.7921
111.9058

CD₂Cl₂

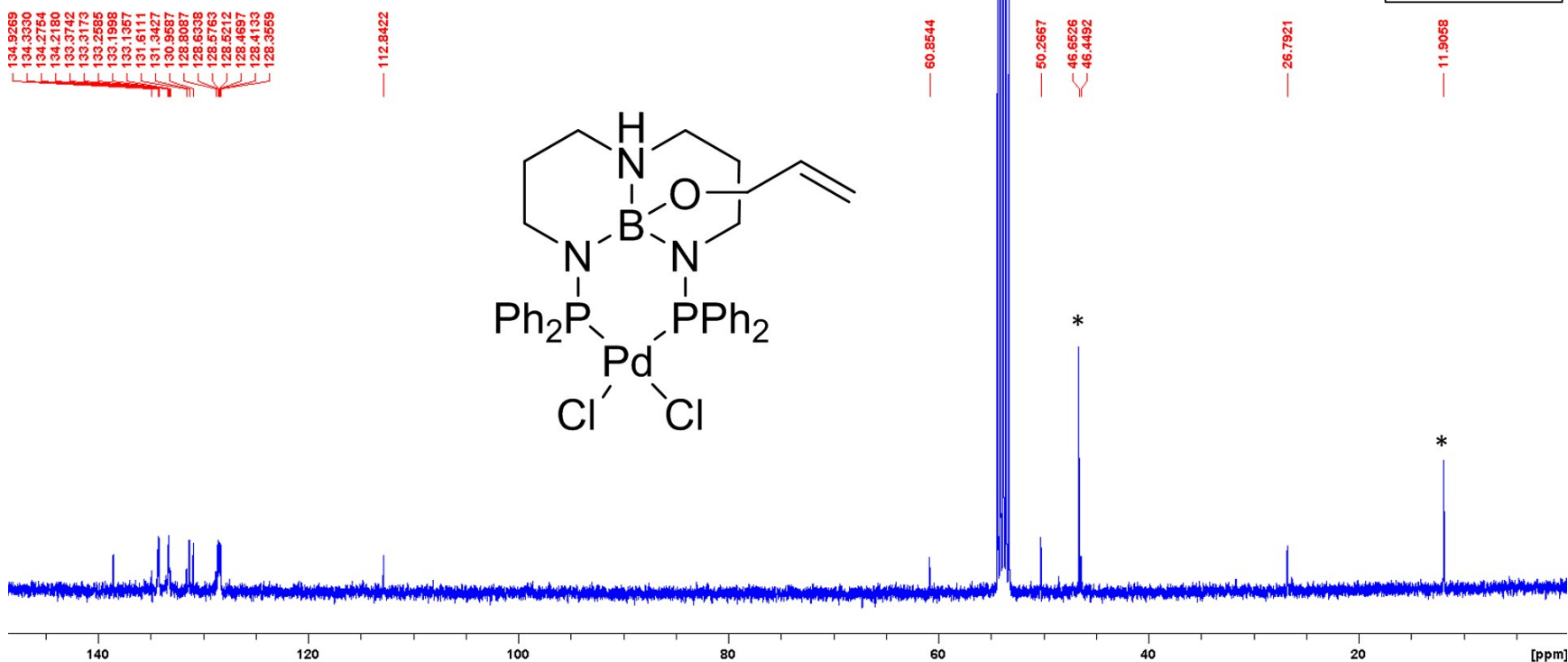


Figure S46. ^{13}C NMR spectrum of ($^{\text{Ph}}\text{TBDPhos-C}_3\text{H}_5\text{OH}$)PdCl₂ (**9**). The * symbol indicates resonances assigned to added NEt₃.

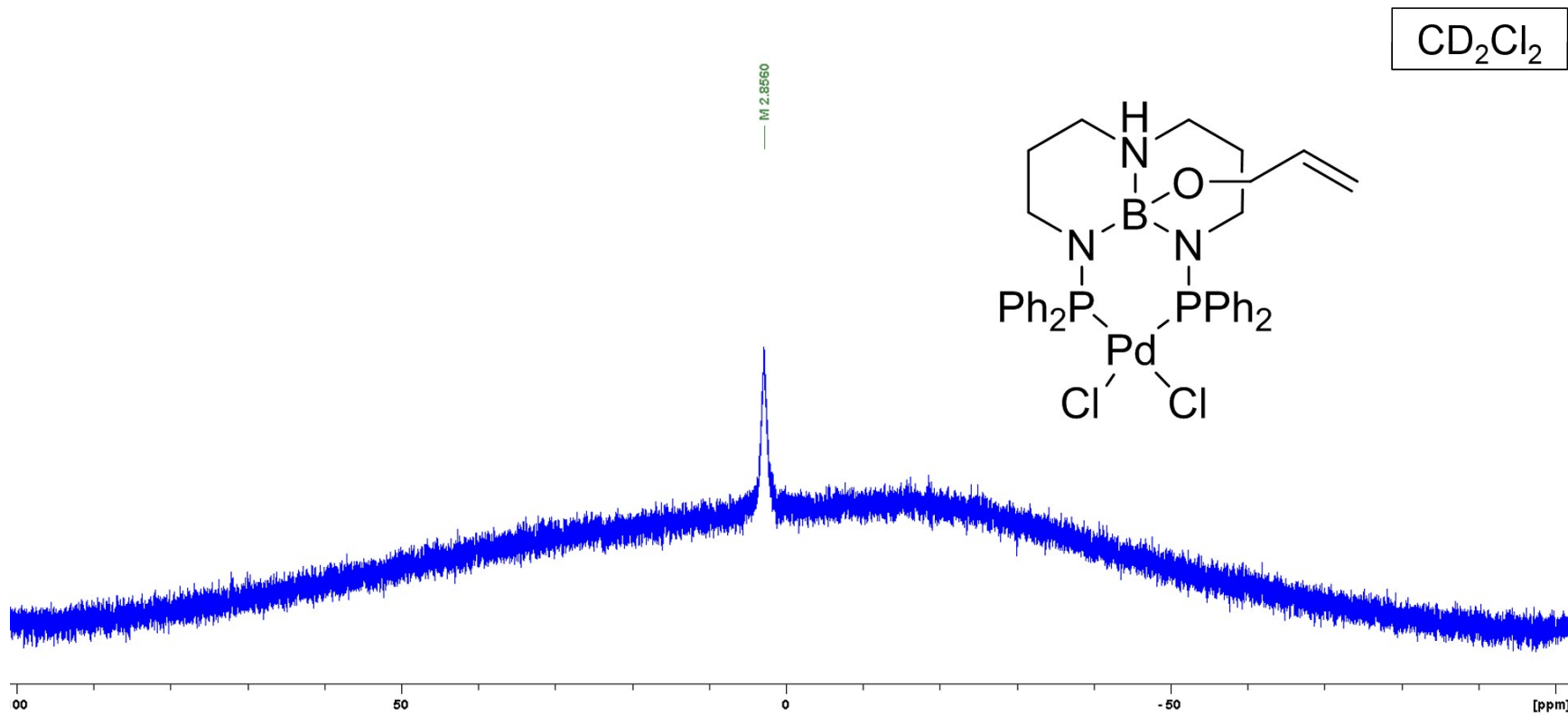


Figure S47. ¹¹B NMR spectrum of (^{Ph}TBDPhos-C₃H₅OH)PdCl₂ (**9**).

CD_2Cl_2

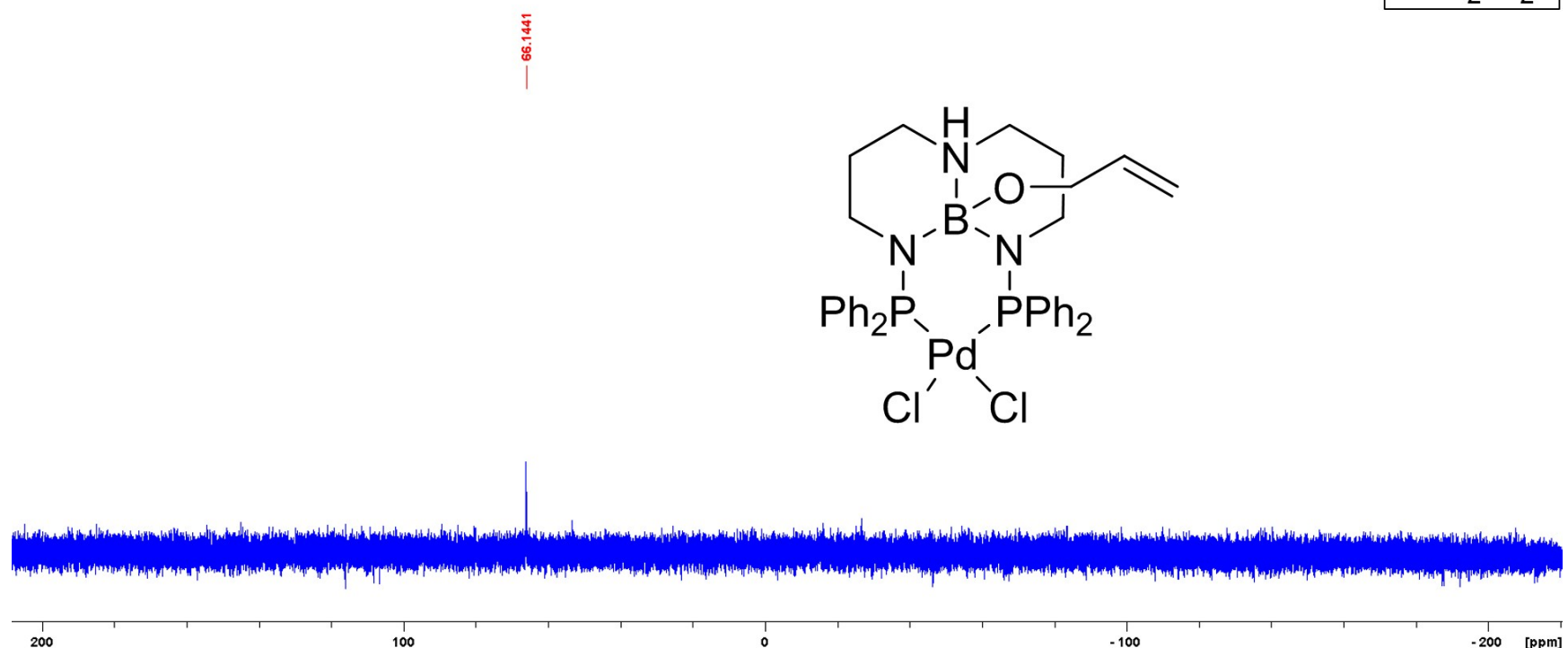


Figure S48. ${}^3\text{P}\{{}^1\text{H}\}$ NMR spectrum of $(\text{PhTBDPhos}-\text{C}_3\text{H}_5\text{OH})\text{PdCl}_2$ (**9**).

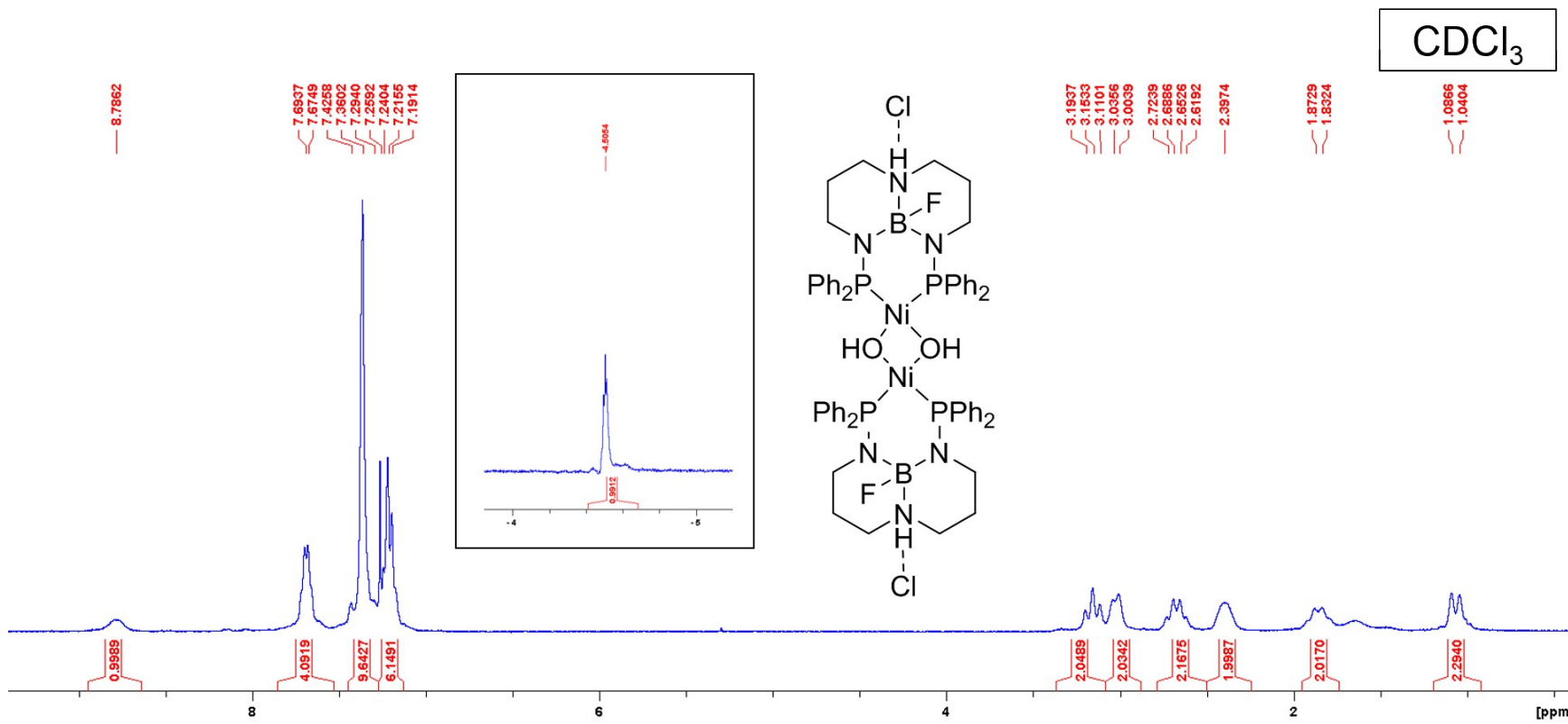


Figure S49. ¹H NMR spectrum of $\{[(^{\text{Ph}}\text{TBDPhos-HF})\text{Ni}]_2(\mu\text{-OH})_2\}\text{Cl}_2$ (**10**).

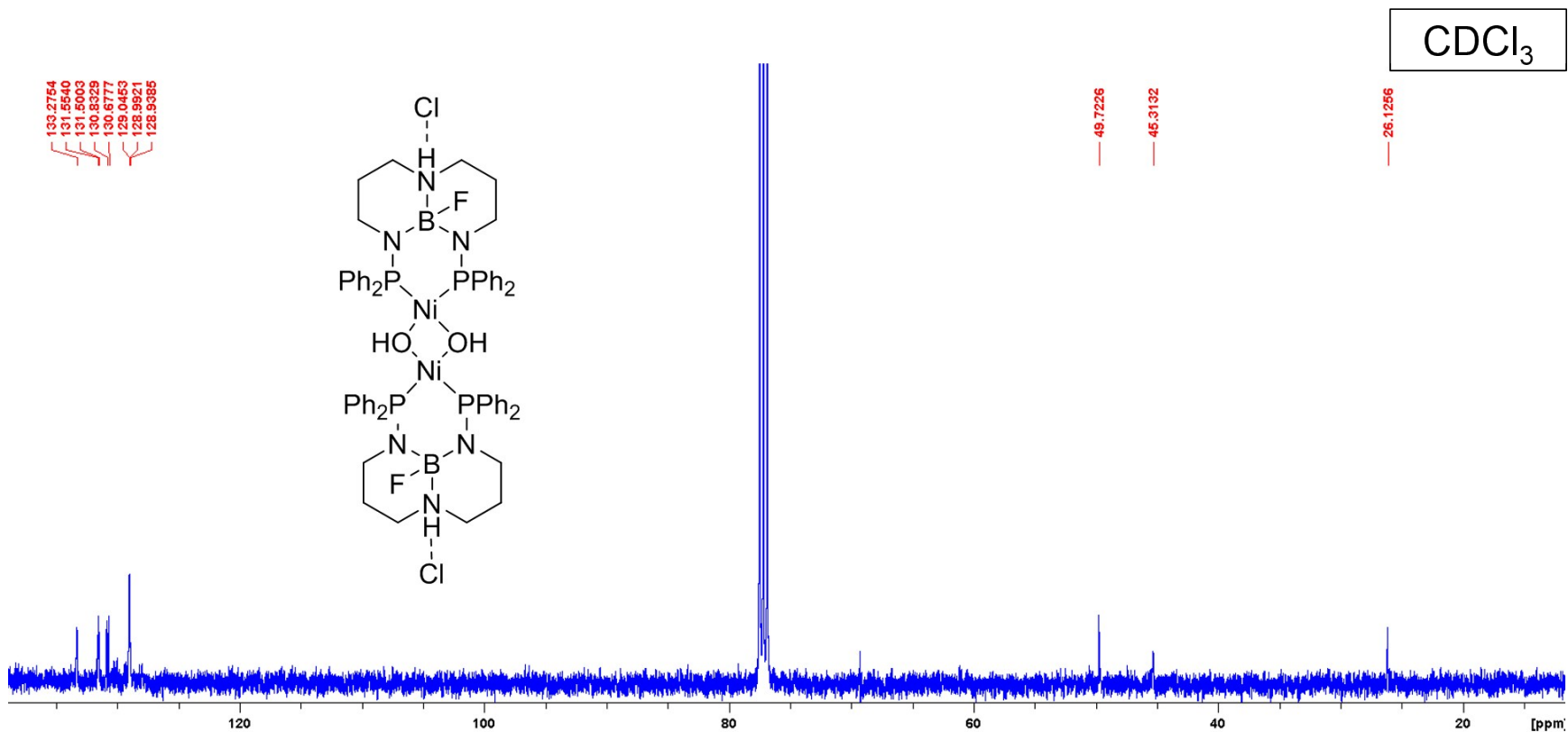


Figure S50. ^{13}C NMR spectrum of $\{[(^{\text{Ph}}\text{TBDPhos-HF})\text{Ni}]_2(\mu\text{-OH})_2\}\text{Cl}_2$ (**10**).

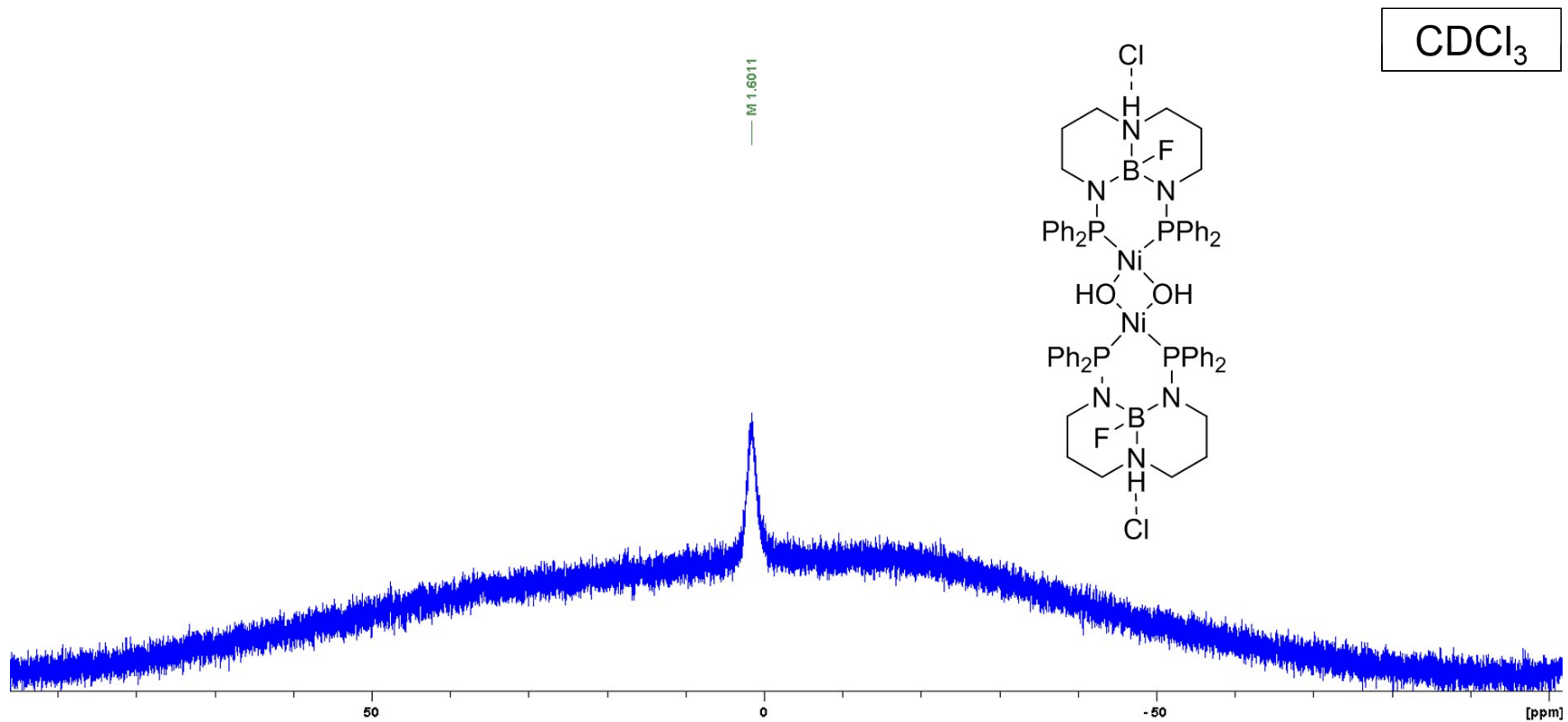


Figure S51. ^{11}B NMR spectrum of $\{[({}^{\text{Ph}}\text{TBDPhos-HF})\text{Ni}]_2(\mu\text{-OH})_2\}\text{Cl}_2$ (**10**).

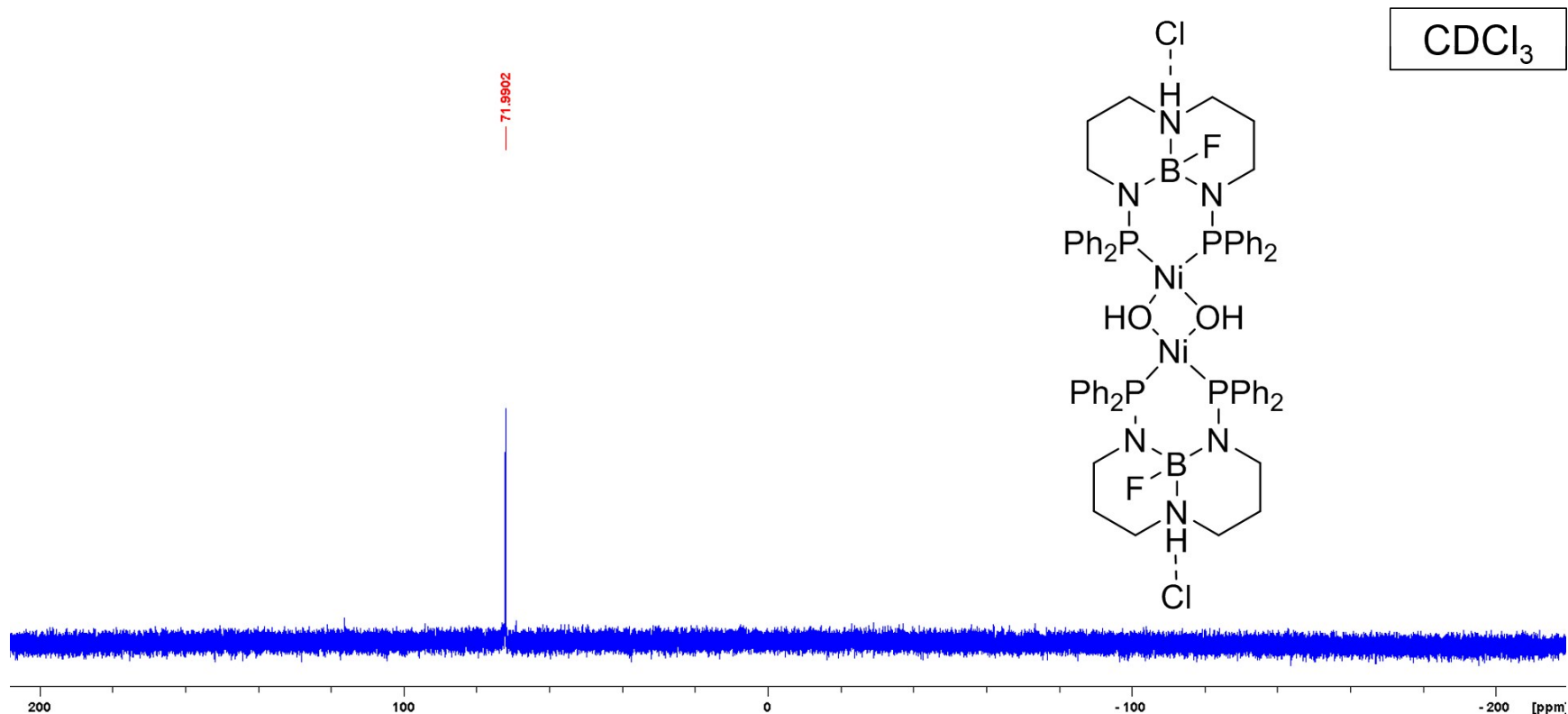


Figure S52. $^{31}\text{P}\{\text{H}\}$ NMR spectrum of $\{[(^{\text{Ph}}\text{TBDPhos-HF})\text{Ni}]_2(\mu\text{-OH})_2\}\text{Cl}_2$ (**10**).

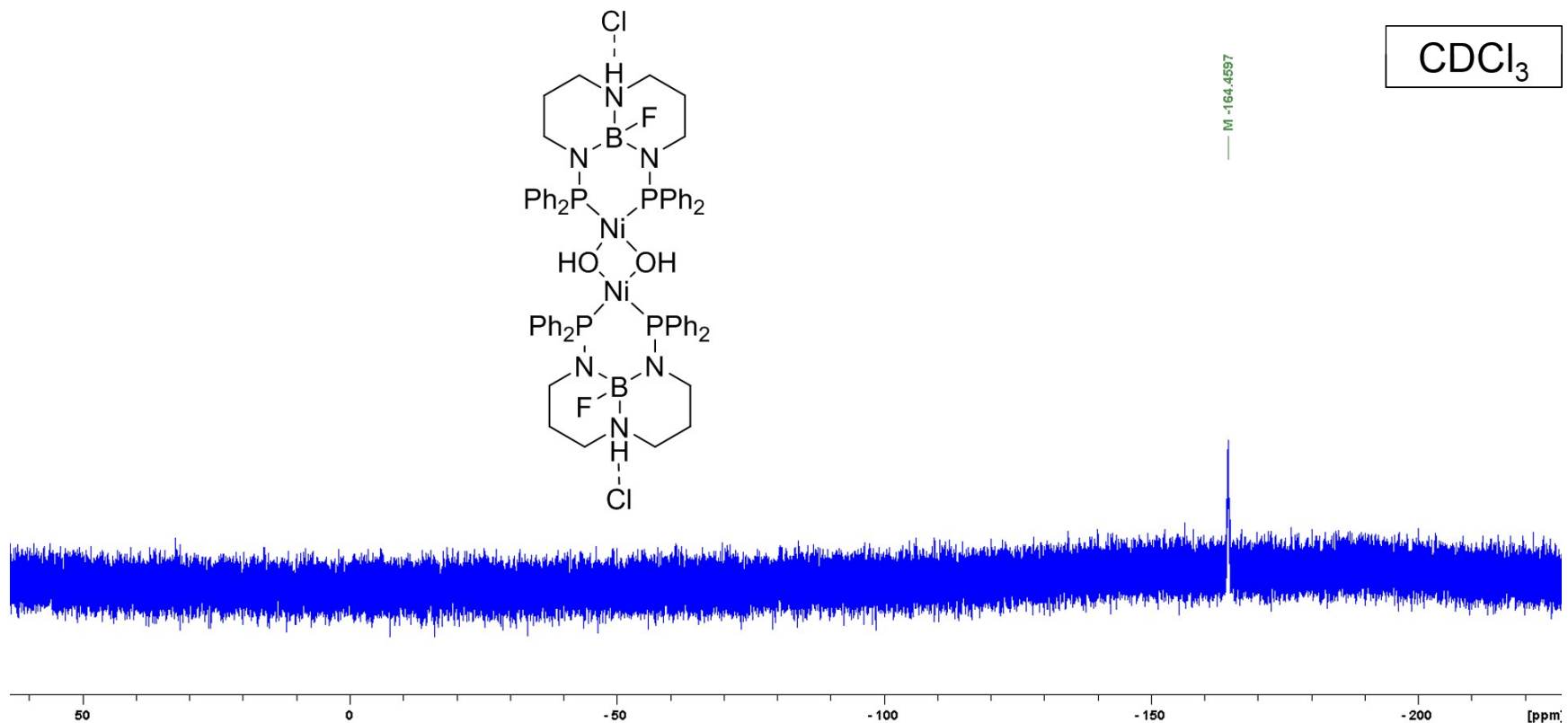


Figure S53. ^{19}F NMR spectrum of $\{[(^{\text{Ph}}\text{TBDPhos-HF})\text{Ni}]_2(\mu\text{-OH})_2\}\text{Cl}_2$ (**10**).